11-3-2014

Penetration through the staple punctures on five N95 respirator models

Daniel E. Medina
University of South Florida, dmedina@health.usf.edu

Penetration through Staple Punctures on Five N95 Disposable Respirators

by

Daniel E. Medina

A dissertation submitted in partial fulfillment
of the requirements for the degree of
Doctor of Philosophy in Public Health
Department of Environmental and Occupational Health
College of Public Health
University of South Florida

Major Professor: Yehia Y. Hammad, Sc.D.
Thomas Mason, Ph.D., M.S.
Steven Mlynarek, Ph.D., C.I.H.
Edwin Rivera, Ph.D.
Rene Salazar, Ph.D., C.I.H.

Date of Approval:
November 3, 2014

Keywords: PPE, Leakage, Head Straps, Aerosol, Filter

TABLE OF CONTENTS

LIST OF TABLES

LIST OF FIGURES

LIST OF SYMBOLS

L_{intact}	Intact leakage
L_{pulled}	Pulled leakage
N_{in}	Number concentration of particles inside the respirator
N_{out}	Number of particles outside the respirator
P_{intact}	Total intact penetration
P_{pulled}	Total pulled penetration
P_{sealed}	Filter penetration
P	Penetration
y	Volume ratio for dilution
F	Fraction of particles in the PSL suspension
VMD	Volume median diameter of the particle size
σ_g	Geometric standard deviation
R	Singlet ratio desired
d	Particle diameter
c	Constant for data transformation
L	Percentage loss
q	Flow rate through the respirator
t	Particle transit time
k	Decay rate
V	Volume
ΔP	Pressure difference
P_a	Ambient pressure
C_{max}	Maximum particle number concentration

LIST OF ABBREVIATIONS

ACGIH	American Conference for Governmental Industrial Hygienist
APF	Assigned protection factor
APR	Air purifying respirator
DVB	Polystyrene divinylbenzene
FFR	Filtering facepiece respirator
MPPS	Most penetrative particle size
NIOSH	National Institute for Occupational Safety and Health
OSHA	Occupational Safety and Health Administration
PEL	Permissible Exposure Limit
PF	Protection factor
PPE	Personal protective equipment
PSLS	Polystyrene latex spheres
PSI	Pressure per square inch
PST	Potassium sodium tartrate
RMANOVA	Repeated measures analysis of variance
SWPF	Simulated Workplace Protection Factor
TLV	Threshold Limit Values
WPF	Workplace Protection Factor

ABSTRACT

Certain N95 FFR models that staple the head straps directly onto filtering material are commercially available. This method of assembly can tear or reduce fiber density in the immediate area surrounding the staple punctures. Five N95 FFR models were evaluated to determine if staple punctures on the filter medium reduce the protection offered by the respirators.

Total penetrations were measured with the staple punctures intact and when stretching the head straps a distance equivalent to a 95% male head circumference. Filter penetration were measured by sealing the staple punctures. Aerosols of 200, 500, and 1000 nm were used to challenge respirators at 28 and 85 Liter/min flow rates. Staple punctures were visually inspected by macrophotography with a light source on the opposing side of the punctures.

Three FFR models had greater mean leakages than the remaining two. However, only two FFR models had statistically significant greater total penetrations than filter penetrations. Pulling the head straps increased total penetration, but was not statistically significant. Filter penetrations were greatest at 85 Liter/min and 200 nm, while leakages were greatest at 28 Liter/min flow rate and 1000 nm.

Leakage through the staple punctures had greater contributions to total penetration than filter penetration allowing a greater percentage of 1000 nm particles into the breathing zone. Leakage was dependent on the tearing of the filter material or the

reduction of fiber density near the puncture, regardless of filter efficiency. Total penetration to filter penetration ratios showed that leakage was greater than filter penetration 15 fold for 1,000 nm. This value is similar to what has been reported for face seal leaks on human subjects. Protection factors were reduced from ~930 to ~60 when the staple punctures created a tear. N95 FFR with stapled head straps that puncture the filter medium should be avoided because they can reduce protection to the user.

CHAPTER ONE:

INTRODUCTION

Respiratory Protection

Respirators are widely used in industry, healthcare, and emergency response situations in order to provide respiratory protection to individuals who may be exposed to an inhalation hazards. The Occupational Health and Safety Administration (OSHA) requires workers to use respiratory personal protective equipment (PPE) for work processes involving particulate inhalation hazards that exceed permissible exposure limits for any particular contaminant (Occupational Safety and Health Standards, 2007). It is the duty of the employer to supply either an atmosphere supplying or air purifying respirator (APR), depending on the contaminant or work processes, to the individual who will be exposed. An APR uses a filter with matted fibers or a charcoal cartridge to remove hazardous particles or vapors from a contaminated atmosphere while atmosphere supplying respirator provide clean air from a line source or tank. The selection requirements for respirator type are provided by OSHA and require the identification and evaluation of the hazard (Occupational Safety and Health Standards, 2007).

Respirator Certification

While OSHA oversees the use and selection of respirators, the National Institute of Safety and Health (NIOSH) is responsible for the evaluation of a respirators and respirator certification (Approval of Respiratory Protective Devices, 1995). Disposable respirators or, filtering facepiece respirators (FFR) that are certified by NIOSH are classified according to the type of aerosols they are intended to be used for and expected minimum efficiency levels provided. The N class respirator is recommended for protection against non-oil solid aerosols only. The R and P class respirators are recommended for protection when oils or liquids are present in the aerosol. The R class respirator is resistant to oily aerosols but should be discarded after a full work shift (8hrs). The P class respirator is oil-proof and can be used for multiple work shifts with exposure to oily aerosols. Each class is also assigned an efficiency level rating of 95, 99, or 100. These rating are based on the percent efficiency of particle removal required to achieve NIOSH certification. The filter efficiencies for each rating correspond to 95%, 99%, and 99.97% respectively.

N95 Filtering Facepiece Respirators

In a survey performed by the NIOSH, 71% of the establishments that require the use of APRs supply their workers with disposable FFR, such as the N95 (NIOSH, 2003). Disposable respirators are convenient and do not require maintenance like the elastomeric cartridge type. They are sought out for their low cost, and ease of disbursement.

N95 head strap attachment methods. Most disposable FFR head straps are attached by stapling the head straps to an outer ledge of the respirator that is not

intended for filtration. Other methods include gluing or welding the head straps to the filter or threading them through a flap that is glued or welded to the filter. However, some of the more economical models of N95 FFR models have their head straps stapled directly onto the filter. This creates a puncture in the medium intended for filtration of workplace aerosols. Currently, NIOSH does not have any requirements on how head straps should be anchored to the respirator filter.

Particle Entry into a Respirator

There are two pathways for particles into the breathing zone of a respirator (Grinshpun et al., 2009). The first and most studied particle pathway into the breathing zone is penetration through filter medium. Particles that enter through this pathway pass through the filter fibers without being collected by the different mechanisms of particle deposition of fibrous filters. These mechanisms of deposition are discussed in a subsequent section of this paper. The second pathway for particle entry into the breathing zone is leakage through gaps between the seal of the FFR and users' face (along the nose, chin, and cheeks).

Determining Leakage

The two pathways can be differentiated by comparing total respirator penetrations on human subjects, on respirators that are partially sealed to a manikin or plate, or respirators with artificial leaks to the filter penetrations of a completely sealed respirator (Grinshpun et. al., 2009; Cho et. al., 2010; Rengasamy & Eimer, 2012). The amount of leakage that occurs can be estimated by determining the filter penetration of

a sealed respirator and subtracting it from the total penetration observed through an unsealed respirator.

Leak Behavior. Studies have shown that the electrostatic charge embedded in disposable N95 FFR create a highly efficient respirator with the most penetrative particle size (MPPS) <100 nm (Martin and Moyer, 2000; Rengasamy, Eimer, & Shaffer, 2009). However, leakage has been shown to be a dominant form of particle entry into a respirator and to correlate with total penetrations while filter penetration do not (Coffey et al, 1998). The fraction of air flow through leaks depends primarily on the size of the leak, and increases as the total flow rate passing through the respirator decreases (Hinds & Kraske, 1987). When small leaks are present, there is a shift in peak leakage to larger particles >900 nm has been observed (Holton, Tackett, & Willeke, 1987; Myers 1986). While the reported MPPS for N95 FFRs are generally <100 nm, one can expected the distribution of particles inside the breathing zone to be determined by leakage.

A third pathway for particle entry. The problem with puncturing the filtering material of an N95 FFR is the potential for leaks in the punctured areas of the filter. As stated previously, party entry into the breathing zone of FFRs is largely determined by leakage rather than filter penetration. Tensions on the staple punctures from pulling the head straps to don (put on) and doff (take off) could stretch or pull the fibers near the staple punctures apart, or even create a tear in the filtering material.

Stapling the head straps of an N95 FFR directly onto the filtering material has the potential to reduce the protection provided by the respirator to the user. In order to provide the highest level of protection to the end user, there is a need to evaluate

respirator components or assembly methods which could inadvertently reduce the integrity of the filter.

Purpose of Study

The purpose of this study is to investigate the amount of leakage through the staple punctures of five N95 FFR models from different manufactures that anchor the head straps onto filter material intended for filtration. Five replicates of each N95 FFR model were tested to determine total penetrations as received (P_{intact}), with tensions on the staple punctures simulating a donned respirator (P_{pulled}), and after sealing the staple punctures with silicone adhesive to determine filter penetration (P_{sealed}). Leakage through the intact and pulled staple punctures (L_{intact} and L_{pulled}) was quantified by subtracting the P_{sealed} from the total penetration of the intact and pulled staple conditions. A repeated measures design was used to reduce the effect of random factors (staple positions, head strap positions, head strap lengths) between respirator replicates. This will eliminate random factors among replicates of the same model when comparing total penetration to filter penetration.

Proposed Research Objectives

The primary focus of this study is to determine if the integrity of five commercially available N95 FFR models is affected by the punctures in the filtering material created from head strap anchoring methods. The following sections provide an overview of the objectives of this study.

Particle leakage through the staple punctures. The null hypothesis is that total penetration when staple punctures are intact or pulled does not differ significantly

from filter penetrations. If the null hypothesis is rejected, then the excess penetration compared to filter penetrations will be considered as leakage.

Increase in leakage when donning the respirator. The null hypothesis is that total penetration from intact staple punctures does not differ significantly from total penetration for pulled staple punctures. If the null hypothesis is rejected, then the excess penetration compared to the intact staple punctures will be considered as additional leakage as a result of donning the respirator.

Conditions of flow and particle size that increase leakage. If either null hypothesis stated above is rejected, a 95% confidence intervals will be used to identify which combination of conditions result in the greatest amount of leakage.

Comparison among respirator models. If either null hypothesis stated above is rejected, 95% confidence intervals will be used to identify differences in leakage between respirators models. The pulled staple punctures will be photographed using an extension tube for macro photography to evaluate possible differences in the staple puncture of the different models used in this study.

Reduction of protection factors. If either null hypothesis stated above is rejected, protection factors will be determined for all staple conditions to investigate if leakage resembles simulated workplace protection factors identified in research studies evaluating respirator fit.

CHAPTER TWO:

LITERATURE REVIEW

Filtration Mechanisms of Fibrous Filters

There are five different known mechanisms of particle deposition that simultaneously work together when filtering air with fibrous filters. The following mechanisms are known as: impaction, interception, settlement, diffusion, and electrostatic attraction. Mechanical filtration encompasses the first four mechanisms. However, settlement contributes an insignificant amount of deposition and is usually ignored. Impaction, interception, and diffusion of particles occur simultaneously and the amount that each contributes towards filtration is particle size dependent.

Particles with diameters greater than 1000 nm are primarily collected by impaction. Greater particle inertia causes it to deviate from the air streamline and collide with a fiber. Interception occurs when the particle does not deviate from the streamline, but is still capture by the fiber. Particles that are too small to be affected by inertia, but too large to be affected by diffusion are captured via interception. The streamline distance from the fiber is shorter than the radius of the particle allowing the particle to come into contact with the fiber while not deviating from the streamline. Diffusion becomes the dominant mechanism of deposition for very fine particles that are pushed around randomly by molecules in air. Particles affected by diffusion can move across a streamline to deposit on a fiber.

Electrostatic attraction is an important mechanism of deposition because it greatly increases the efficiency of the filter without increasing the breathing demand of the user. Today all disposable N95 FFR rely on the electrostatic charge placed on its fibers to achieve certification. However, the embedded charge can degrade when the filter is exposed to high temperature and humidity, organic liquid aerosols, and ionizing radiation (Hinds, 1999). When these conditions are present, the use of an R or P class FFR is more appropriate. Some of the methods used to charge the fibers are known as turboelectric charging, corona charging, and charging by induction. These are explained in greater detail by Brown (1995).

Respirator Charge

Studies have shown that the efficiency of a N95 FFR is greatly reduced when the charge is removed from the fibers. When the fiber charge is removed the MPPS shifts upwards towards the 300 nm range (Martin & Moyer, 2000). In their study, Martin and Moyer tested N95 FFR before and after dipping them in isopropanol to remove the embedded charge. The MPPS ranged from 50 to 100 nm and shifted towards 250 to 350 nm after removing the charge of the FFR. Similar findings were obtained by Rengasamy et al. (2009). Plebani, Listrani, Tranfo, and Tombolini have shown that exposure to paraffin oil aerosol also degrades electrostatic deposition and shifts the MPPS upward (2012). Mostofi et. al. used two different particle measurement techniques and reported the MPPS to be under 100nm for both methods (2012). Rengasamy and Eimer have reported the MPPS on N95 FFR to be 50nm (2011). Majority of these studies agree that the MPPS remains the same under different flow rates for N95 FFR with an embedded charge in the filter fibers.

Challenge Aerosols

Aerosols produced and used for determining the efficiency of a respirator in a laboratory setting are known as challenge aerosols. A common method of producing a challenge aerosol is by atomizing or nebulizing a liquid suspension containing particles of a desired size. Some common materials that have been used to create aerosols include polystyrene latex spheres (PSLS), potassium sodium tartrate (PST), polystyrene divinylbenzene (DVB), or sodium chloride (Hinds, 1999). Challenge aerosols can be prepared with monodisperse or polydisperse distributions, meaning they can have a uniform distribution of single sized particles or a distribution spread across many particle sizes. A monodisperse challenge aerosol is often preferred because aerosol filtration properties are highly dependent on particle size (Hinds, 1999).

According to Hinds, there are three different problems that may occur when using PSLS (1999). The size of the spheres may differ from what the manufacturer reports, the creation of doublets and chains of PSLS which may result when multiple spheres are nebulized in a single droplet, and the formation of particles of an undesired size by the residue of the PSLS stabilizer in empty droplets.

Aerosol Treatment

Today's particulate air purifying respirators have a negative and positive charge embedded in the filter fibers of the filters to capture contaminants with greater efficiency while reducing the pressure demand of the user. The efficiency of a charged filter may be affected by the general charge of the aerosol cloud (Hinds, 1999). Neutralizing the charge of the aerosol cloud results in an equal number of positively

and negatively charged particles. This creates a more challenging aerosol for filter penetration tests of electrostatically charged respirators (Approval of Respiratory Protective Devices, 1995). This neutral distribution of aerosol charge is referred to as the Boltzmann equilibrium state (Hinds, 1999).

NIOSH Test Method for N95 Certification

NIOSH requires and performs an evaluation of respirators performance for certification of N95 FFRs. Up to 20 replicates of each FFR model are challenged with a sodium chloride aerosol during the evaluation (Approval of Respiratory Protective Devices, 1995). A 2% sodium chloride solution in distilled water is nebulized and the aerosol is charge neutralized to the Boltzman equilibrium. The count mean diameter of the aerosol cloud is 75 nm with a standard deviation of 186 nm. The test is conducted in an airtight testing chamber at a flow rate of 85 Liters/min through the respirator medium. Respirators are preconditioned at 38°C ± 2.5°C and 85% ± 5% relative humidity for approximately 24 hours prior to testing. The test is performed at 25°C ± 5°C and a relative humidity of 30% ± 10%.

The protocol requires the first three replicates to be loaded with 200mg ± 5mg of sodium chloride aerosol. If the respirator efficiency remains constant or increases over the first 12 minutes of the test, then the initial reading for the remaining respirators is sufficient. Otherwise, the remaining respirators must be tested. Filters that have 95% or less efficiency are removed and remounted to the test plate to ensure no leakage has occurred due to improper sealing of the respirator on the test plate. If the excessive leakage has been eliminated, then the sample is considered invalid and another respirator must be tested. The highest penetration observed over one-minute

intervals is recorded as the maximum penetration level of the filter. For certification, the minimum efficiency of each filter tested must be greater than 95%.

N95 Use in Healthcare Settings

N95 FFRs are prevalent in healthcare settings to prevent transmission of airborne infectious diseases. A large portion of particles expelled by a cough are in the respirable size range. Lindsley et. al., reported that up to 68% of the particles per cough emitted by a person infected with influenza are in the respirable range (2012a). Furthermore, under low ventilation conditions, particles emitted by a cough can travel in a plume across a room and expose people to high concentrations of infectious particles (Lindsley et. al., 2012b).

Lore et. al. has reported the physical filtration of MS2 influenza virus through respirators behaves similarly to that of sodium chloride particles (2012). Hogan et. al. has observed MS2 virions in aerosol particles in the MPPS reported for mechanical and electrostatic filtration (2005). In a similar study, Noti et. al., found that 19.5% of the recovered virus from a cough aerosol were in particles under 100 nm (2012). Viruses infect a person by count, not by mass. Therefore this information suggests that a poorly fitted N95 FFR could place the wearer at an increased risk of infection. The CDC recommends individuals who cannot avoid close contact with an infectious person to use an N95 FFR (CDC, 2009). Surgical masks are considered inadequate respiratory protection against pandemic influenza (OSHA, 2009).

Protection against Nanoparticles

Exposure to fine particles has been known to cause respiratory health effects (WHO, 1999). Advances in technology have increased the demand for processes involving nano-materials, therefore increasing the likelihood of exposure to nanoparticles in the workplace. NIOSH has expressed concern and has set a focus in research on exposure to nanoparticles (NIOSH, 2009).

Nano-materials are often produced in powder forms and can easily become aerosolized when handling material. Nanoparticles are also created unintentionally in work processes that require energy. Welding, grinding, sanding and combustion processes are common sources of nanoparticles. However, exposures to secondary sources of nanoparticles are typically greater than 100 nm due to agglomeration or continuing condensation (Vincent & Clement, 2000). The potential toxicity of the materials being used or created may warrant respiratory protection.

The emerging field of nanotechnology has had a large impact on the use of respirators. Reference standards such as permissible exposure limit (PEL) set by OSHA or recommendations such as threshold limit values (TLV) set by the American Conference of Governmental Industrial Hygienist (ACGIH) are determined according to mass concentrations. While the mass concentration of an exposure may be in compliance with the PEL or under the TLV, exposures to particle count may still be very high. The larger surface area of the particles allows more contact between the contaminant and lung tissue and can deposit deeper in the lungs where biological clearance mechanisms are inefficient. Oberdorster, G., Oberdorster, E., and Oberdorster, J. report that particle surface area or particle count is better predictor of

health effects than aerosol mass (2005). The lack of standards specific to engineered nano-materials may create a preference to use respiratory protection (Schulte et. al., 2008).

Studies on Filter Performance and Leakage

Most recent studies evaluating disposable respirators have focused on filter performance when challenged against nanoparticle and sub micrometer particle sizes. Few studies have reported particle penetration through the filter media of N95 respirator in excess of 5% (Balazy et. al., 2006). Due to the high efficiency of electret and charged fiber filters studies have focused on FSL into the respirator. Leakage refers to particles that enter the breathing zone of a respirator through streamlines along the face seal or tear on the filter material (Myers, Allender, Plummer, & Stobbe, 1986). Therefore, the filtration mechanisms working on particle deposition are reduced when leakage occurs. Penetration is an appropriate term to describe particles that enter the breathing zone of a FFR through an uncompromised section of filtering material and still escape one the different modes of deposition (impaction, interception, gravitation, diffusion, electrostatic attraction) (Rengasamy & Eimer, 2011).

Studies investigating leakage through FFR use filter penetration as a baseline to quantify additional inward leakage of particles into the respirator (Rengasamy & Eimer, 2012; Chen & Willeke, 1992; Hinds & Kraske, 1987; Grinshpun et. al., 2009). These studies have investigated the behavior of leakage through artificial leaks in the respirator, or excess penetration into the breathing zone of human subjects.

Holton et. al. has shown that the geometry of the hole or tear in the filter will affect leakage, suggesting that a slit or narrow gap in the face seal results in less leakage than a circular hole (1987). Chen and Willeke have also reported that leakage through a single circular hole was greater than multiple smaller holes or a slit with an equivalent cross-sectional area (1992). These studies have also demonstrated that lower flow rates through the respirator are associated with higher leakage.

In these studies, the greatest leakage was identified at 5 Liter/min and it decreases with increasing flow rate. Cho et. al. found that most particle penetration into the respirator occurs through the face seal leakage, which varies with breathing flow rate and also particle size (2010). Recently, Rengasamy and Eimer have confirmed the effect of flow rate on leakage and suggest that penetration levels through a sealed respirator are a good indicator of leakage when artificial leaks were introduced (2014). Additionally, a respirator with a high pressure drop is expected to have greater particle leakage (Chen, Ruuskanen, Pilacinski, & Willeke, 1990).

The size of the leak has been shown to influence which particle size has the highest peak. Holton et. al. reported that as the size of the leak decreases, the total particles leaking decreases but a greater percentage of larger particles leak (1987). Grinshpun et al. has reported that 1000 nm particles are more likely to leak than 100 nm particles through the face seal on human subjects (2009).

Much of the immediate concern with leakage on N95 FFR and other disposable respirators has to do with fit (Lofgren, 2012). Brosseau observed gaps along nose area in 80% of the participants in a fit test study (2010). Another study on 211 subjects showed that 69% fail a qualitative fit test (Burgess & Mahingaidze, 1999). Reponen, Lee, Grinshpun, Johnson, and McKay reported that the overall passing rate for fit

testing on four N95 FFR models was 67% (2011). However, passing a fit test does not guarantee the wearer and adequately fitting respirator (Coffey et. al., 2004). The majority of these studies report that lack of proper training on the correct method of donning a respirator is likely to influence failures to achieve a good fit.

Assigned protection factors (APF) represent the minimum protection that a specific type of respirator must provide a user after fitting (OSHA, 2009). OSHA has set an APF of 10 for N95 FFR. An APF of 10 suggests that up to 10% of airborne particles could enter the breathing zone when properly fitted and worn (Rengasamy, Eimer, King, & Shaffer, 2008). When evaluating WPFs for microorganisms with mean aerodynamic particle size less than 5 micrometers, Lee et. al. reported that more than 50% of the measured WPFs were below the APF for FFRs (2005).

Stapled Head Straps

N95 respirators are available in many designs and produced by different manufactures. Depending on the model and the manufacturer, the head straps are attached to the respirator using different methods. Higher end models have the head straps threaded through a flap that is glued to the respirator which allows the respirator to hang from the neck when not in use. More economical models commonly have the head straps stapled or glued directly to the filtering material or to an outer edge that is not used for filtering air. Models that have their head straps stapled directly onto the filtering material create a puncture through the FFR.

Multiple donning can stress FFR components such as head straps, strap attachments and adjustable nose pieces (Bergman et. al., 2012). For respirators with

staple punctures, the stress from multiple donning has the potential to tear a hole between the filter and the staple which may allow particles to leak, reducing the protection provided by the FFR. The variability in head strap length and elasticity can vary the stress placed on respirator components when donning (Bergman et al., 2012). Brosseau, reported that users adjust the head straps incorrectly 25% of the time (2010).

Respirator Reuse

Currently, there are no time restraints on the use of N95 FFR, and the number of maximum safe reuses is not specified (NIOSH, 2014). Respirators are usually discarded when there is visible damage or if there is an increase in the pressure demand that is not tolerable by the user. As particles build up on the filter the pressure demand will increase. As the pressure drop across the respirator increases, the amount of flow through leaks increases (Brown, 1995). The economic incentive of reusing respirators may further increase leakage through the face seal.

CHAPTER THREE:

METHODOLOGY

Research Design

Twenty-five NIOSH approved N95 respirators, or subjects, with head straps that are stapled directly onto the filtering material were selected for this study. One of the respirators models selected has also been selected as part of the U.S. Strategic National Stockpile (FDA, 2010; Viscusi et al., 2011). The subjects were segregated into 5 groups, according to respirator model. Each group was assigned a letter for identification.

Inspection of Staple Punctures

The staple punctures on the five different models of N95 FFR were inspected using a light source on the opposing side of the filter. The head straps where pulled to simulate a donned respirator during inspection. In some models, the filter material adjacent to the staple puncture allows more light through in comparison to the other areas of the filter material. This suggests that the fiber density in the immediate area is reduced. The staple puncture on one of the five N95 FFR models created a tear in the filter medium. Tension from multiple donning/doffing (putting on/taking off) and prolonged use of the respirator over the course of several days or weeks of use has the potential to further affect the integrity of the filter material near the staple punctures.

Figure 1 shows the staple punctures on three of the N95 FFR models selected for this study.

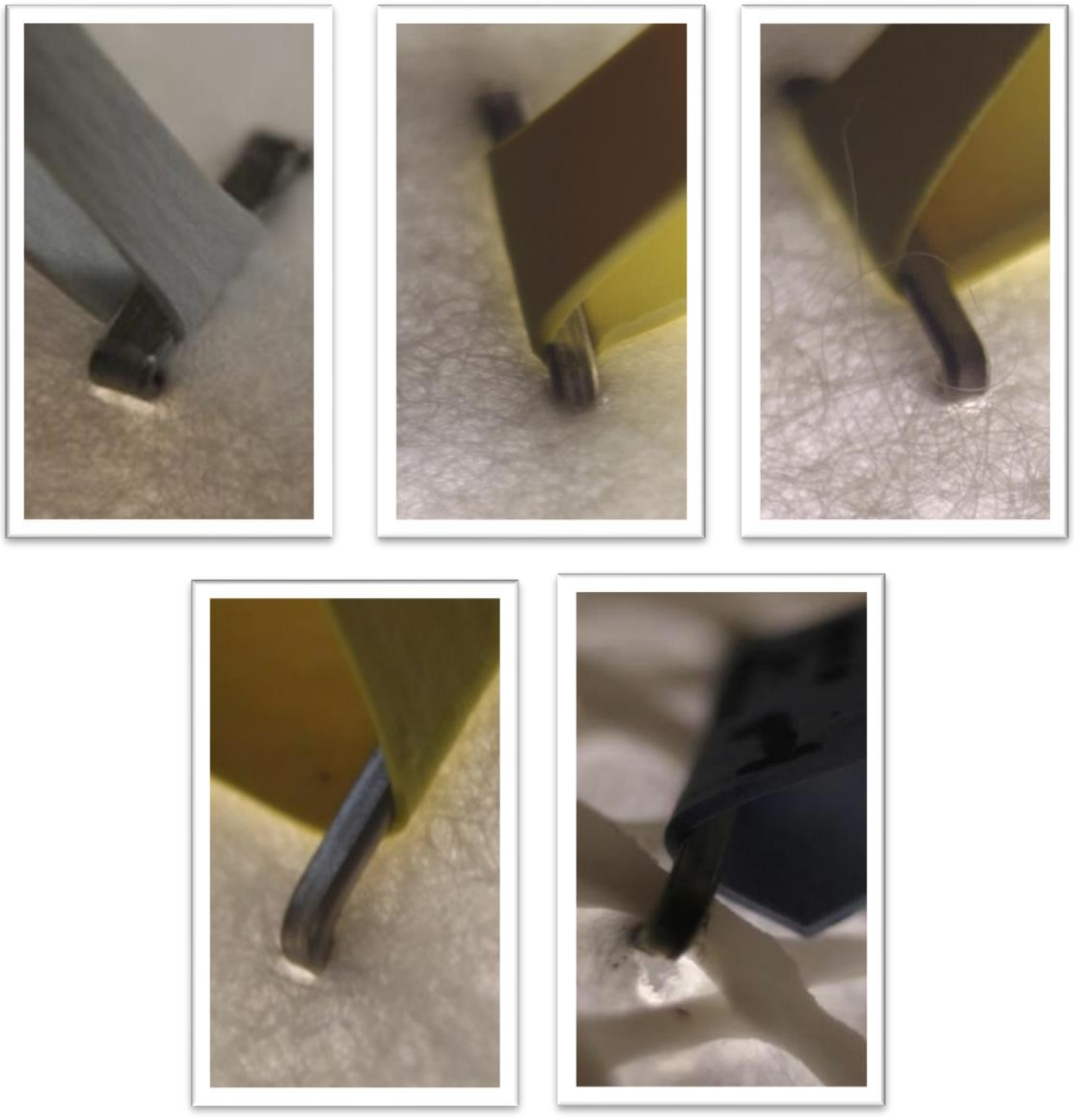

Figure 1. Staple punctures on N95 FFR with pulled head straps.*

**From top left to bottom right: N95 group A, B, C, D, & E.*

Measurement of Total Penetration and Filter Penetration

Respirator penetration was obtained by using number concentration of particles inside and outside the respirator.

$$P\% = \left(\frac{N_{in}}{N_{out}}\right) \times 100\%$$

Where:

P% is the percentage of particles that penetrated the respirator

N_{in} is the number of particles inside the respirator

N_{out} is the number of particles outside the respirator

Subjects were challenged using 200, 500, and 1,000 nm Polystyrene latex spheres (Magsphere Inc.), at 28 and 85 Liter/min flow rates and three staple conditions. The staple conditions: intact, pulled, and sealed corresponded to the respirator tested 'as received' (intact staple), simulating a 'donned respirator' (pulled staple), and simulating a respirator with head straps affixed using a different method that does not puncture the filter (sealed staple). A minimum one hour time period was allowed to pass after stretching the head straps prior to testing the respirator under pulled condition. After the staple punctures were sealed, the adhesive was allowed to cure for a minimum of 60 minutes.

Summary of variable conditions. The different variables and subsequent levels are presented in below. Penetration was approximated using the average of 5 observations. A total of 2,250 (25×3×3×2×5) individual penetration calculations were made in this study.

Number of subjects = 25 (5 groups divided by FFR model)

Staple conditions = 3 (Intact, Pulled, Sealed)

Particle sizes = 3 (200 nm, 500 nm, 1000 nm)

Flow rates = 2 (28 Liter/min, 85 Liter/min)

Number of observations per data point = 5

Estimation of Leakage

The total penetration through the respirator under sealed staple condition, or P_{sealed}, represents the typical penetration for the filter. The P_{intact} and P_{pulled} are composed of the filter penetration, plus the amount of particles that leak through the intact or pulled staple punctures. The difference between P_{intact} to P_{sealed} gives an estimate of the amount of leakage through the intact staple punctures (L_{intact}). Likewise the difference between and P_{pulled} and P_{sealed} gives an estimate of the amount of leakage through the pulled staple punctures (L_{pulled}).

$$P_{intact} - P_{sealed} = L_{intact}$$

$$P_{pulled} - P_{sealed} = L_{pulled}$$

Where:

P_{intact} = Total Intact Penetration

P_{pulled} = Total Pulled Penetration

P_{sealed} = Filter Penetration

L_{intact} = Intact Leakage

L_{pulled} = Pulled Leakage

Estimation of Total Penetration to Filter Penetration Ratios

Intact and pulled leakage can also be investigated by examining intact and pulled to sealed ratios. These ratios estimate the number of particles that leak through the staple punctures for each particle that passes through the filter.

$$P_{intact} / P_{sealed} = \text{Intact Leakage to Filter Ratio}$$

$$P_{pulled} / P_{sealed} = \text{Pulled Leakage to Filter Ratio}$$

A ratio that represents no leakage would be less than 1. A ratio greater than 1 would indicate that for every particle that passes through the filter medium, the number of particles that leak through the staple puncture is equal to that ratio.

Estimation of Protection Factors

Protection factors are calculated by dividing the outside concentration of a respirator to the inside concentration. PFs that are measured in the field, while the user is performing work, are referred to as workplace protection factors (WPF). PFs that are measured in a laboratory setting, while the user is performing a series of set exercises, are referred to as simulated workplace protection factors (SWPF). The observed PFs offered by the N95 FFR models in this study were determined from the penetration values obtained.

$$PF = \frac{100\%}{P\%}$$

The PFs in this study do not resemble SWPF factors because they are not actually donned by a human subject. However, identifying the reduction in PF allows for comparison to studies on respirator fit. Table 1 shows the corresponding penetration percentage that enters the breathing zone of an FFR for different PFs.

Table 1. Protection factors and their corresponding filter penetrations.

Protection Factor	Total Penetration (%)
10	10.0
20	5.0
50	2.0
100	1.0
200	0.5
300	0.3
400	0.3
500	0.2
1000	0.1

Table 2. EPA recommended short-term exposure values for inhalation for males and females combined.

Activity Level	Age Group (years)	Mean (LPM)	95th Percentile (LPM)
Sedentary / Passive	21 to 30	4.2	6.5
	31 to 40	4.3	6.6
	41 to 51	4.8	7
	51 to 61	5	7.3
Light Intensity	21 to 30	12	16
	31 to 40	12	16
	41 to 51	13	16
	51 to 61	13	17
Moderate Intensity	21 to 30	26	38
	31 to 40	27	37
	41 to 51	28	39
	51 to 61	29	40
High Intensity	21 to 30	50	76
	31 to 40	49	72
	41 to 51	52	76
	51 to 61	53	78

Data from EPA Exposure Factors Handbook, 2011

Flow Rate Selection

The flow rates used in this study are 85 Liter/min and 28 Liter/min which are representative of the NIOSH testing conditions and mean inhalation rate for an adult under moderate activity level respectively. Table 2 shows the EPA recommended values for inhalation rates when considering short term exposure samples (EPA, 2011). NIOSH performs testing for filter certification at a flow rate of 85 Liter/min simulating heavy workload conditions.

Aerosol Generation

Diluted suspensions of the different size PSLS were prepared prior to testing each staple condition. Water used for creating dilutions was filtered with a Barnstead Nano Diamond water filtration system. The Collison nebulizer and all glassware used to create the dilutions were cleaned in an ultrasonic bath and then rinsed with nano-filtered water.

Polystyrene Latex Sphere Dilutions

Dilutions were designed so that 95% of the droplets created would only hold one PSL sphere. When multiple PSL spheres are housed in one droplet, the particles may stick together which could create chains of agglomerates and affect the desired particle size distribution. The guideline calculation to achieve 95% droplets with a single PSL spheres inside was given by Raabe (1968).

$$y = \frac{F(VMD)^3 e^{4.5 ln^2 \sigma_g}}{(1-R)d^3}\left[1 - \left(e^{ln^2 \sigma_g}\right)/2\right]$$

Where:

y is the ratio of the new volume to the old volume

F is the fraction of particles in the PSL suspension

VMD is the volume median diameter of the particle size

σ_g is the geometric standard deviation

R is the singlet ratio desired

d is the diameter of the particle

For the diluted 200 nm suspension used in this study, 10 µL of 15% by volume PSLS suspension was mixed with 150 mL of nano-filtered water (1/15000 dilution factor). A 20 mL portion of the resulting suspension was placed inside a collision nebulizer for testing. For 500 nm diluted suspensions, 10 µL of 15% by volume PSLS suspension was mixed with 20 mL of nano-filtered water (1/2000 dilution factor). For the 1,000 nm diluted suspension, 50 µL of 15% by volume PSLS suspension was mixed with 20 mL of filtered water (1/1000 dilution factor).

Figure 2. Aerosol generation.*

**From left to right: Collison nebulizer, silica diffuser, charge neutralizer.*

Respirator Preparation

Each respirator was sealed using a silicone adhesive to a faceplate for at least 12 hours prior to testing. The faceplate was sealed to a plenum that allows sampling inside (downstream) the respirator. Visual inspections for leaks between the silicone adhesive and the face plate were conducted prior to sampling. If reapplication of adhesive was needed the respirator was allowed to dry to the minimum setting time recommended by the silicone adhesive manufacturer (60 minutes). After visual inspection, the respirator and faceplate were placed in the center of the testing chamber.

Respirator Sampling Mount

In order to sample inside (downstream) the respirator, it was sealed to a sampling mount prior to testing. The sampling mount was composed of two parts: the plenum and the faceplate. Both pieces were constructed out of acrylic. A hole was made in the faceplate to allow air entering the respirator through and into the plenum. The respirators were sealed to the faceplate, allowed to dry, and inspected. Afterwards the faceplate was sealed to the plenum using petroleum jelly and clamps. This allowed the removal of the faceplate for easier removal of the respirator once testing was completed.

The sampling mount was tested for leaks prior to performing any tests. A faceplate with no hole was used to seal to the plenum. The particle counter was connected to one of the sampling ports on the plenum. The particle counter calibration filter was connected to the other port on the plenum. The resulting system allowed air

to enter into the plenum through the calibration filter. No leaks were identified when using petroleum jelly to seal the faceplate to the plenum.

The size of the plenum and rear of the mounting plate allowed stretching the head straps a fixed distance selected to represent the circumference of 95 percentile male head of the current American workforce (Zhuang & Bradtmiller, 2005). The mounting of the respirator to the faceplate was selected to resemble the NIOSH respirator mounting method.

Sampling error can occur when measuring the concentration inside the respirator (Myers et. al., 1986; Holton et. al., 1987). When leaks are present, streamlining of particles may occur inside the respirator (Myers et. al., 1986). These studies suggest that particles entering the breathing zone of the respirator do not mix well and the location of the sampling port will produce different results when leaks are present. The plenum was used to avoid sampling error due to the streamlining effect. The sampling port for the particle counter was positioned at the back of the plenum to increase the distance from the face of the respirator.

Particle Counter

A laser diode particle counter (Lasair II 110, Particle Measurement Systems) with the capability to measure particles ranging from 100 nm to 5,000 nm was used in this study. The particle counter is intended for use in cleanrooms to monitor and maintain ISO clean room standards. The transit time of a particle through the laser beam and the concentration of particles can create coincidence losses where the counter may not register every particle that has passed through. When more than one particle passes the laser at the same time, only one event is counted. Assuming the

particle counter has a transit time of 6.2 µs, coincidence loss was estimated according to the manufacturer:

$$L\% = [1 - exp(-q \times t \times C_{max})] \times 100\%$$

Where:

L is the percentage of loss

q is the flow rate through the respirator [m^3/sec]

t is the particle transit time [µs]

C_{max} is the maximum particle number concentration [number/m^3]

The coincidence loss of the particle counter is approximately 5% when the cumulative number concentration is 17.7 x 10^6 counts/m^3. Estimating the coincidence loss allows estimation of particle count when the concentration exceeds the capability of the instrument.

Test Chamber

The test chamber used for this study was constructed from glass and aluminum. It has approximate dimensions of 50x50x50 cm^3 and volume of 125 liters. There are many similar sized chambers that have been used successfully in recent studies. Balazy et. al. has shown that a chamber of relatively small volume (34 liters) can be successfully used to predict respirator performance in the workplace (2006). Rengasamy & Eimer have used an acrylic chamber measuring 30x30x30 cm^3 (2011). Eshbaugh, Gardner, Richardson, and Hofacre, used a chamber with dimensions of 75x75x60 cm (2008).

Identification of Leaks in Test Chamber

Leaks have the potential to alter the distribution of the test aerosol inside the chamber. Leakage could occur around the door, sampling ports, and other connections. To identify leaks in this study, the chamber was sealed and placed under positive pressure. The air intake filter cartridges were sealed with a PVC cap with a barb connector to allow for sealing the chamber or directing treated air into the chamber.

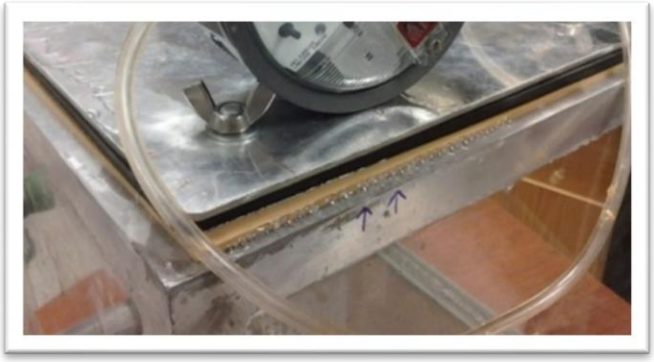

Figure 3. Air bubbles from leak in test chamber door.

Leakages were investigated using soap and water over the areas and components of the chamber that could potentially leak. This method identified several leaks around the door and some of the quick disconnect ports. The edges of the chamber were warped around the door area and the initial gasket used was too rigid to produce an adequate seal. Uneven surfaces were filled in with epoxy putty and sanded down to create a smooth and level edge for the gasket. The door gasket was replaced with a softer closed cell foam rubber, which improved the seal. Teflon tape was wrapped around the area of the quick disconnect valves for a tighter fit.

Determination of test chamber leak rate. An acceptable leak rate is 2% or less of the total flow through the chamber (Mokler and White 1983). After identifying and sealing all leaks in the positive pressure test, a negative pressure test was conducted. The leak rate was calculated as follows:

$$leak\ rate = kV\left(\frac{\Delta P}{P_a}\right)$$

Where:

k = decay rate [min^{-1}] = 0.089

V = volume of chamber [Liters] = 125

ΔP = pressure difference [mm Hg] = 3.74

P_a = ambient pressure [mm Hg] = 760

The decay rate, *k*, is the slope of the pressure decay inside the chamber starting at 2"H_2O, (3.74 mm Hg). Figure 4 shows the pressure decay for the negative pressure test. The total flow through the chamber was 100 Liter/min. The leak rate is 0.048 Liter/min which was well under 2% of the total flow through the chamber (2.5 Liter/min).

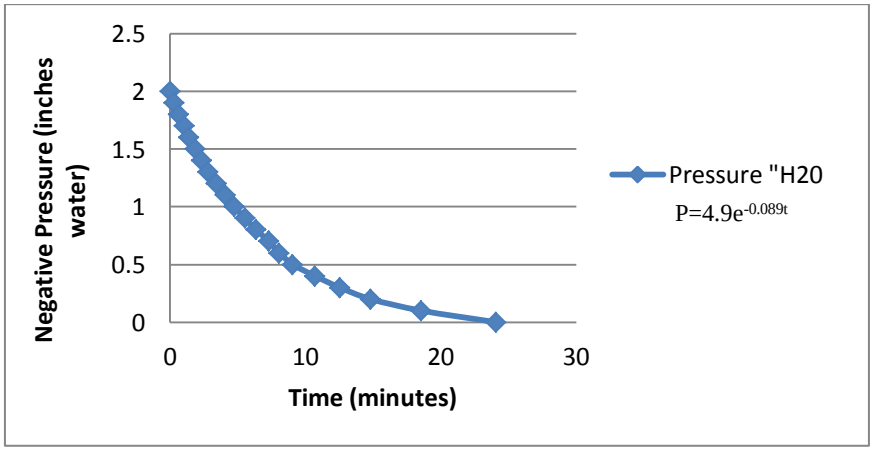

Figure 4. Pressure decay rate of test chamber.

Experimental Flow

A flow diagram of the experimental setup is provided in Figure 5. Compressed nitrogen (A) at 20 PSI (B) was passed through a HEPA filter (C) into a 3-jet Collison nebulizer (D) with a known PSL dilution. The aerosol exiting the nebulizer at 6 Liter/min was diluted by exhausting 3.5 Liter/min using a critical orifice (E) and pump (F) prior to entering the silica gel diffuser (G). The critical orifice was made by crimping a hypodermic needle until a desired flow rate was obtained. A HEPA filter was connected to the critical orifice to prevent clogging. The diluted aerosol was passed through a silica gel diffuser (G) and then directed through a Krypton-85 charge neutralizer (H). The silica gel diffuser ensures that only PSL spheres enter the chamber by diffusing the water vapor form the aerosol. The charge neutralizer creates equilibrium of positive and negative charges in the aerosol cloud.

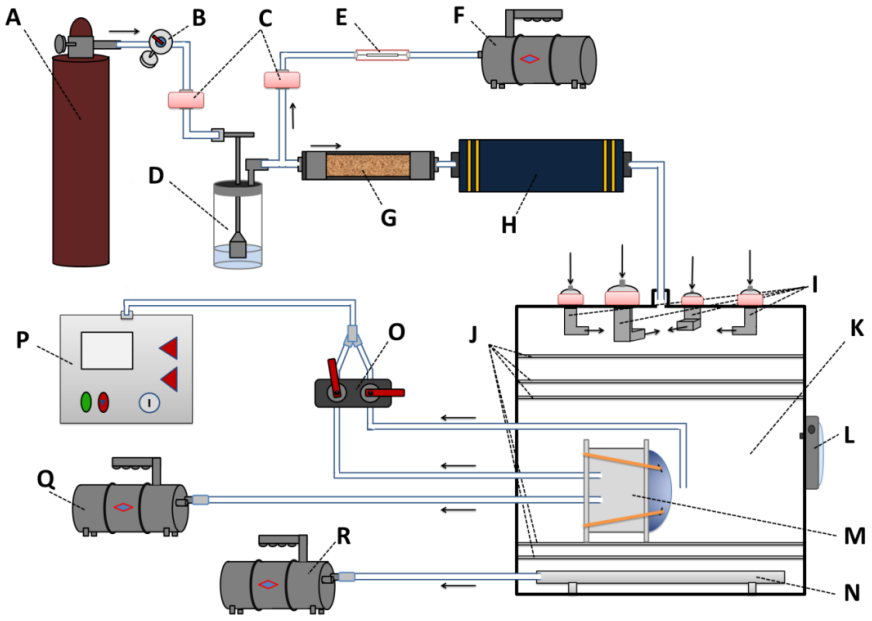

Figure 5. Experimental design flow diagram.*

**A-Compressed Nitrogen; B-Pressure Gauge; C-HEPA Filter; D-Collison Nebulizer; E-Critical Orifice; F-Pump; G-Diffusion Dryer; H-Charge Neutralizer; I-Clean Air Intake; J-Diffuser Panels; K-test Chamber; L-Pressure Gauge; M-Respirator Mounting Plate; N-Exhaust Manifold; O-Switch Valve; P-Particle Counter; Q-Pump; R-Pump.*

The aerosol enters through the top center of the chamber (K) and is mixed by clean air entering through four P100 filter cartridges (MSA, Pittsburgh, PA). Each clean air intake port has an elbow (I) that directs clean air to the center of the chamber and ensures good mixing of the challenge aerosol. Three diffuser panels (J) below the mixing area maintain a uniform distribution through the chamber. The respirator mounting plate sits on top of two additional diffuser panels. An exhaust manifold (N) underneath the bottom diffuser panel exhausts air from the chamber at 40 LPM which was directed into a lab hood by a pump (R). A Magnahelic (Dwyer Instruments, Inc.) pressure differential gauge (L) was used to monitor the pressure inside the chamber during leak testing of the chamber. A change in pressure during testing signals a disruption of the flow in the system. A particle counter (P) was connected to a switch valve (O) which allowed sampling inside and outside the respirator sampling mount plenum (M). The particle counter operated at 28.3 Liter/min. To achieve a flow rate through the respirator of 85 Liter/min, a third pump (Q) was connected via a quick release valve to the respirator mount plenum. The pump flow rate was set to 57.7 Liter/min. The higher flow of 85 Liter/min was selected to resemble NIOSH testing conditions. When the pump (Q) was disconnected from the plenum, the resulting flow through the respirator was 28.3 Liter/min, which is the flow rate that particle counter operates under. To maintain the total flow through the chamber equal during low and high flow testing, 28 Liter/min and 85 Liter/min respectively, the pump (Q) was connected to the chamber exhaust manifold when not connected to the respirator sampling mount plenum. The total flow through the chamber during testing conditions resulted in approximately 97.7 Liter/min.

All flow rates were inspected using a mass flow meter prior to and after testing each respirator to ensure that all flow rates are within ± 3 Liter/min of the target flow rate. Relative humidity and temperature were checked before and after each respirator. Temperature in the chamber maintained at 70°F ± 3°F and relative humidity at 65% ± 10%. The silica diffusion dryer was inspected prior to testing and replaced when gel color indicated it was saturated.

The chamber was allowed to purge for 10 minutes prior to aerosol generation. After purging the chamber, the Collison nebulizer was pressurized to 20 PSI and aerosol generation started. The system was allowed to run a minimum of 10 minutes to allow the concentration inside the chamber to stabilize. The respirator mount plenum was also purged for 2 minutes prior to collecting data. Testing on each respirator, for the 18 conditions, took approximately 12 hours.

Statistical Analysis

IBM SPSS Statistics v.22 was used for the statistical analysis of this study. A Repeated Measures Analysis of Variance (RMANOVA) was conducted for the P_{filter} (sealed staple) of each N95 FFR group, as well as when including P_{intact} and P_{pulled} (intact and pulled staple). Significant increases in total penetrations compared to P_{filter} were evaluated using 95% confidence intervals. Two additional RMANOVA were conducted to compare leakages, as well as P_{pulled}/P_{filter} and P_{intact}/P_{filter} ratios among the respirator groups. A Shapiro-Wilk test and Levene's test were used to test for the assumption of normality and equality of error variance. Multiple comparison post hoc tests between groups were performed using the Bonferonni method for insight but negated due to the use of marginal means for all variables used in this study.

Significant interaction terms that include staple condition were considered for identification of variables that influence leakage.

The following RMANOVA were conducted for this study. All comparisons were performed using 95% confidence intervals with the consideration of all variables and their sub-levels for analysis.

1- RMANOVA for P_{filter}: how do respirators perform (between, within)?
2- RMANOVA for P_{intact}, P_{pulled}, P_{filter}: are leakages significantly greater than filter penetration (within)?
3- RMANOVA for L_{intact} and L_{pulled}: are leakages different between the models (between)?
4- RMANOVA for P_{pulled}/P_{filter} and P_{intact}/P_{filter}: does the amount of particles leaking to passing through the filter differ between the models and conditions (between, within)?

Diagnosis of Data (Assumptions)

The Shapiro-Wilk test showed that the data were non-normal for groups of respirator models (n=5) and all subjects (n=25). A Levene's test showed that the data were homogenous for groups of respirator models, but heterscedastic for all subjects (n=25). Repeated measures ANOVA are robust against violations of normality but less so when equality of variance is violated. The results of the Shapiro-Wilk test of normality and Levene test of homogeneity are presented in Appendix A, Table. A1. When considering the median instead of mean, there were equal variances among all subjects.

Data Transformation

Common methods of transformation include (in order of strength of transformation): a square root, logarithmic, and reciprocal transformation (Osborne, 2002). The reciprocal transformation was used in this study, because it was found that it eliminates most outliers in the data set.

The use of power transformations will produce unwanted effects on observations that range between 0 and 1 (Osborne, 2002). According to Osborne the effect of transformation is maximized by shifting the distribution so that the minimum value is anchored at 1 (2002). The constant, c, was selected to shift the distribution so that there were no values within 0 and 1 and that the lowest penetration value observed was anchored at 1. The transformation calculation used was:

$$1/(P+c)$$

The data remained non-normal after reciprocal transformation according to the Shapiro-Wilk test. However, after transformation, an improvement was observed in the normality of the distribution and outliers were eliminated (fig. A1 & fig. A2). When using reciprocal transformations, small values become very large and large values become very small. The data are mirrored, and cannot be interpreted as log transformed data, which can be plotted on a log plot. After conducting the RMANOVA, the results and 95% CI were back-transformed for interpretation. The back-transformed means and 95% CI were plotted using Microsoft Excel 2010. The calculation used for back-transformation was:

$$(1/P) - c$$

CHAPTER FOUR:

RESULTS

The results of the RMANOVA are reviewed and main effect terms and interactions terms including staple are summarized in this chapter. The results of the RMANOVA for intact, pulled, and sealed staple penetrations are discussed in more detail in Appendix B. The results for pairwise comparisons of 95% CI including all variables are discussed in this chapter.

Filter Penetrations

Filter penetrations (P_{sealed}) were estimated by taking five measurements of concentration inside and outside the N95 respirators at each of the conditions of particle size, and flow rate, while the staple punctures were sealed. P_{sealed} for the five models are shown in figures 6 and 7. Comparisons of 95% confidence intervals were made to determine significant differences among the respirators and between the different levels of particle size and flow rate. Table B1 shows the mean P_{sealed}, standard error, and 95% confidence intervals for all respirator groups and the marginal means respirator groups and can be found in Appendix B.

The RMANOVA for filter penetrations showed a significant main effect for particle size and interaction for particle size×flow rate for all respirator groups (Table

3). Flow rate was a significant main effect for Respirator Groups B, C, and D. Groups A and E did not have a significant main effect for flow rate.

Table 3. Repeated measures ANOVA results for filter penetration (sealed staple condition).

	Respirator Group				
Variable	**A**	**B**	**C**	**D**	**E**
Particle Size	0.005*	<0.000*	<0.000*	0.001*	0.002*
Flow Rate	.106	0.001*	0.001*	0.002*	.086
Particle Size × Flow Rate	0.001*	<0.000*	0.001*	<0.000*	0.003*

*Statistically significant ($p<0.05$)

Low Flow Filter Penetrations

At low flow, P_{sealed}, was less than 1% for all particle sizes for all respirator groups (fig. 6). Group D had the highest filter penetration for all particle sizes 1%, 0.44%, and 0.43% (200, 500, 1000 nm respectively). Group E had the lowest filter penetration for all particle sizes 0.28%, 0.17%, and 0.11% (200, 500, 1000 nm respectively).

Comparison of 95% CI for mean P_{sealed} showed that differences between filter penetrations at 200 nm were significantly greater than 500 nm and 1,000 nm particle sizes in Group D ($p<0.05$). Furthermore, filter penetration in Group D at 200nm was significantly greater than the other groups ($p<0.05$). Filter penetrations for all other groups did not differ significantly as a function of particle size. All respirator groups showed a minimal increase in filter penetrations with decreasing particle size.

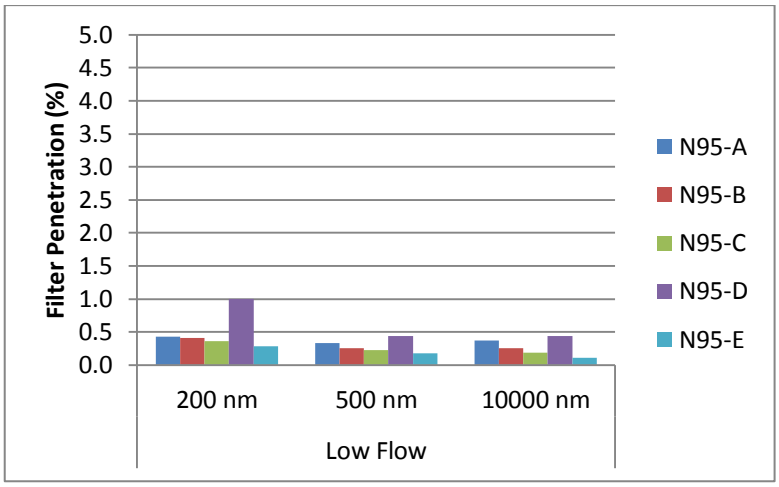

Figure 6. Filter penetrations for the N95 FFR groups at 28 Liter/min constant flow rate.

High Flow Filter Penetrations

At high flow P_{sealed} were under 5% for all respirator models (fig. 7). Group D had the greatest filter penetrations for all particle sizes 4.93%, 1.89%, .69% (200, 500, 1000 nm respectively). Group A had the lowest filter penetrations for 200 and 500 nm particle sizes (.84%, .42%, respectively). Group E had the lowest filter penetration for 1,000 nm particle size (.17%).

Comparison of 95% CI for mean filter penetrations showed that filter penetrations were greater at the higher flow rate for 200 and 500 nm particle size ($p<0.05$) for all respirator groups. In Group D, filter penetration for 200 nm were significantly greater than 500 nm and 1,000 nm particle sizes ($p<0.05$). Furthermore, in Group D, filter penetration at 200nm was significantly greater than all other groups ($p<0.05$). In Group A, filter penetration for 200 nm was significantly lower than all other groups. Filter penetration for all groups were highest at 200 nm and decreased with increasing particle size.

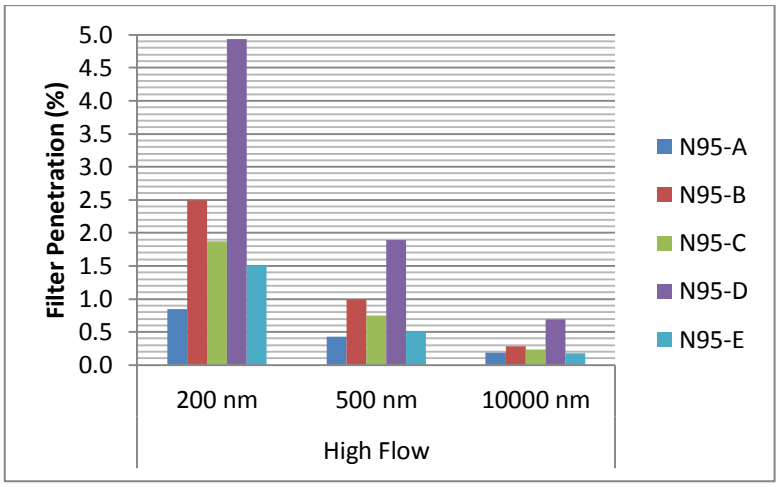

Figure 7. Filter penetrations for the N95 FFR groups at 85 Liter/min constant flow rate.

Intact, Pulled and Sealed Staple Penetrations

A RMANOVA that included all staple conditions (intact, pulled, and sealed staples) was performed. The results for the RMANOVA are presented in Table 4. Staple condition was found to be a significant main effect for all respirator groups except Group B ($p<0.05$). Interaction for staple×size was significant for Group C. Interaction between staple×flow rate was significant for Group D and E ($p<0.05$). Interaction including all terms staple×size×flow rate was significant for Group A ($p<0.05$). Table B1 shows the mean penetrations, standard error, and 95% confidence intervals for all respirator groups and the marginal means respirator groups and can be found in Appendix B.

Table 4. Repeated measures ANOVA results for intact and pulled penetrations and filter penetrations.

	Respirator Group				
Variable	**A**	**B**	**C**	**D**	**E**
Staple	0.038*	.080	0.098*	0.013*	0.004*
Particle Size	0.005*	<0.000*	<0.000*	0.001*	0.002*
Flow Rate	.106	0.001*	0.001*	0.002*	.086
Staple × Particle Size	.518	.776	0.039*	.666	.120
Staple × Flow Rate	.057	.182	.793	0.024*	0.001*
Particle Size × Flow Rate	0.001*	<0.000*	0.001*	<0.000*	0.003*
Staple × Particle Size × Flow Rate	0.040*	.396	.063	.415	.466

*Statistically significant
$p<0.05$

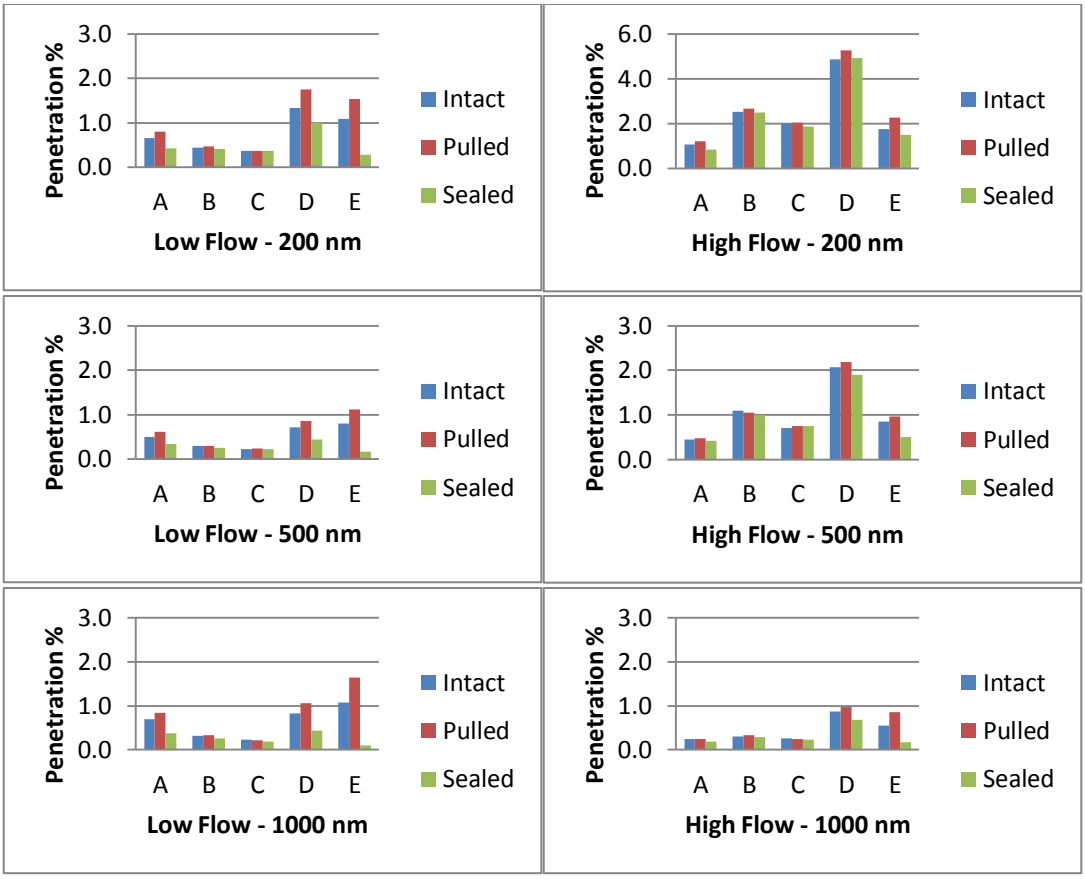

Figure 8. Total penetrations for intact, pulled, and sealed staple conditions.*

**Left column shows flow rate of 28 Liter/min and right column shows flow rate of 85 Liter/min. The top, middle, and bottom rows show the 200, 500, and 1,000 nm particle sizes.*

Leakage

Leakage for intact and pulled staple punctures was determined by subtracting the intact and pulled penetrations to the sealed penetrations. Comparisons of 95% confidence intervals were made to determine which conditions (particle size, and flow rate) result in significant increase of total penetration through the intact and pulled staple punctures. Comparisons were also made between intact and pulled staple conditions to determine if stretching the head straps significantly increased leakage through the staple punctures. The mean leakages for all N95 respirator groups are presented in figures 9-12 below. Table B2 shows the L_{intact} and L_{pulled} , standard error, and 95% confidence intervals for all respirator groups and the marginal means respirator groups and can be found in Appendix B. Pulled leakages were generally greater than intact leakages for all particle sizes and flow rates, but the differences were not statistically significant.

Low Flow Leakage

Under low flow, Groups A and E had significant leakage with respect to filter penetrations ($p<0.05$). In Group A, leakage was significant for particles of 500 and 1000 nm for both intact and pulled staple conditions ($p<0.05$) (fig. 9 and fig. 10). In Group E, leakage was significant for all particle sizes under intact and pulled staple conditions ($p<0.05$). The greatest leakages for Group A and Group E were observed under low flow and pulled staple conditions (.46% and 1.53% respectively).

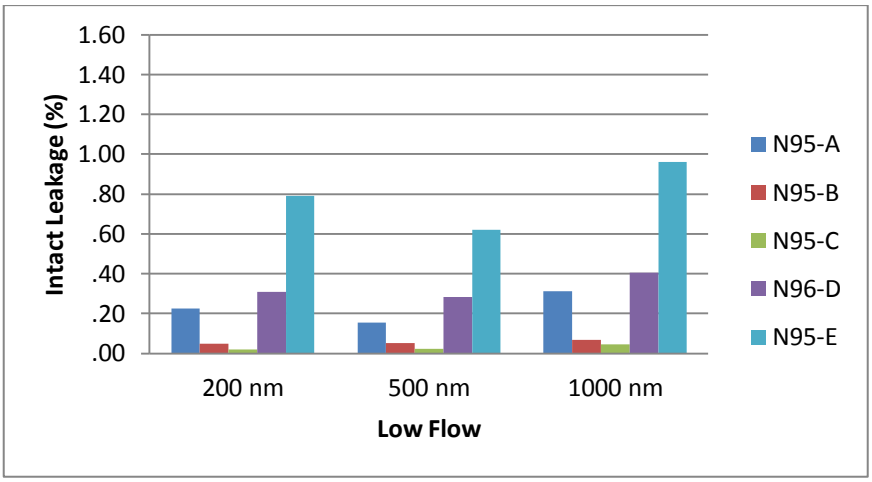

Figure 9. Intact leakage for the N95 FFR groups at 28 Liter/min constant flow rate.

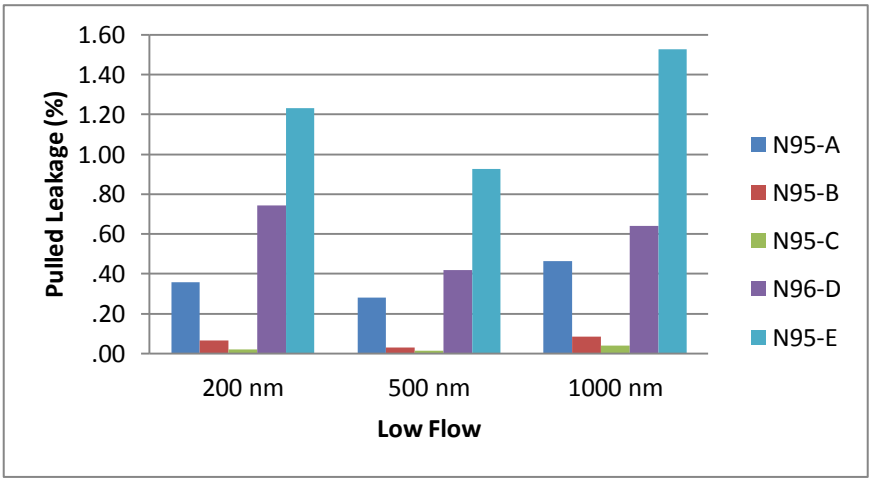

Figure 10. Pulled leakage for the N95 FFR groups at 28 Liter/min constant flow rate.

High Flow Leakage

Under high flow, all respirator groups showed the greatest leakage at 200 nm and pulled staple condition (fig. 12). However, when staples where intact, Group D and E had the greatest amount of leakage at 1,000 nm (fig. 11). This is similar to what is described by Myers, suggesting that when the size of a leak is reduced, particle size distribution shifts to larger particles (1986). This may be due to the changes in inertial

losses related to the size of the hole (Holton et al., 1987). Group E was the only respirator group that showed significant leakage for pulled staple condition. This was only observed for 1,000 nm particles (.68%) ($p<.05$). However, the largest mean leakage in Group E under pulled staple condition was at 200 nm particle size (.79%). This could be due to higher variability of both filter penetrations and total penetration through the staple punctures at the 200 nm particle size. Intact leakages were not statistically significant for any of the respirator groups.

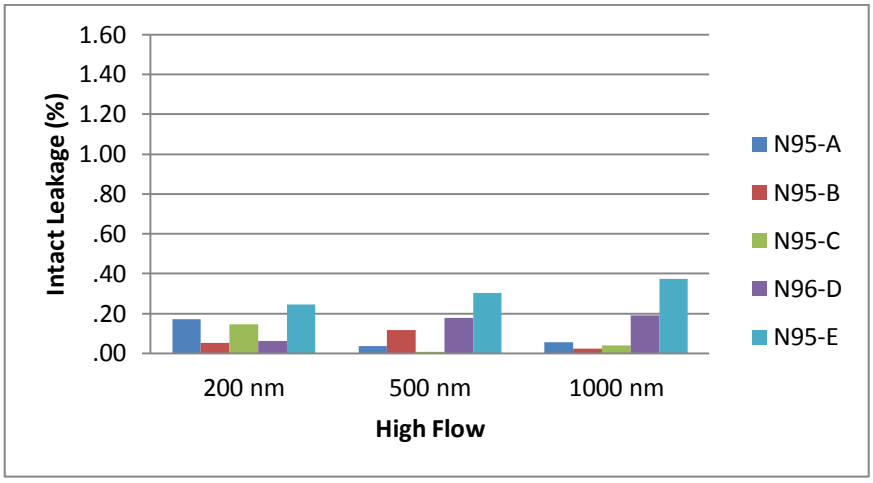

Figure 11. Intact leakage for the N95 FFR groups at 85 Liter/min constant flow rate.

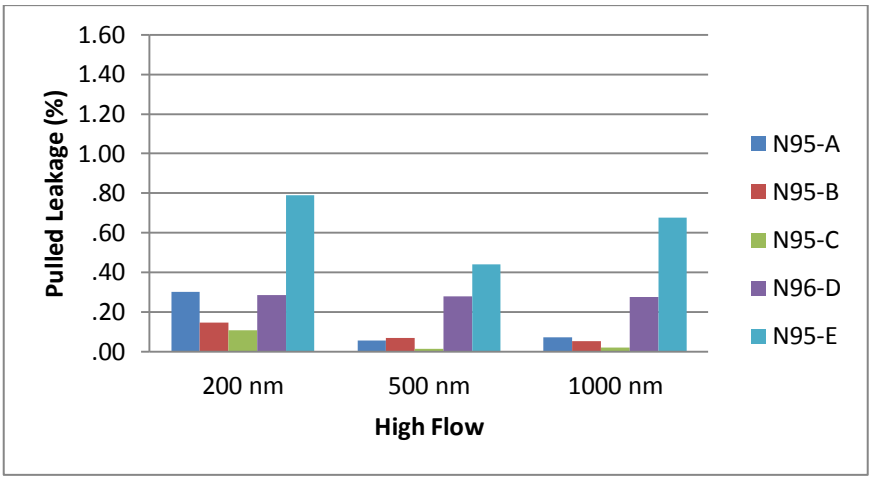

Figure 12. Pulled leakage for the N95 FFR groups at 85 Liter/min constant flow rate.

Total Penetrations (Intact and Pulled) to Filter Ratios

The total intact and total pulled penetration to filter penetration ratios (P_{intact}/P_{sealed} and P_{pulled}/P_{sealed}) give insight as to how many particles passed through the staple punctures for each particle that passed through the filter of the respirator. A total penetration to filter penetration ratio of 1 would indicate that excess particles are not entering through the staple punctures. A total penetration to filter ratio greater than one, would indicate how many particles pass through the staple punctures for each particle that passes through the filter.

A RMANOVA was performed for the total penetration to filter ratios. The results for the RMANOVA are presented in Table 5. There are only two levels of staple condition for the total penetration to filter ratios (intact and pulled). Staple condition was found to be a significant main effect for Group D ($p<0.05$). Particle size had a significant main effect for Group E ($p<0.05$). Flow rate had a main effect for all groups except Group C. Interaction for staple×size was not significant for any groups. Interaction between staple×flow rate was significant for Group D ($p<0.05$).

Interaction including all terms staple×size×flow rate was not significant for any groups.

Table 5. Repeated measures ANOVA results for total penetration to filter ratios.

	Respirator Group				
Variable	**A**	**B**	**C**	**D**	**E**
Staple	.104	.446	.726	.002*	.091
Particle Size	.149	.401	.126	.130	.016*
Flow Rate	.010*	.033*	.307	.004*	<0.000*
Staple × Particle Size	.844	.424	.453	.239	.355
Staple × Flow Rate	.137	.993	.555	.029*	.257
Particle Size × Flow Rate	.728	.385	.024*	.975	.242
Staple × Particle Size × Flow Rate	.836	.931	.731	.613	.380

*Statistically significant
Staple composed of intact and pulled variable levels

Comparisons of 95% confidence intervals were made to determine which conditions including all variables tested (staple condition, particle size, and flow rate) result in significant differences among the respirators and between the variable levels tested. Table B3 shows the mean total penetration to filter ratios, standard error, and 95% confidence intervals for all respirator groups and the marginal means respirator groups and can be found in Appendix B.

Low Flow Total Penetration to Filter Ratios

Figures 13 and 14 show the mean P_{intact}/P_{sealed} and P_{pulled}/P_{sealed} ratios under low flow. Generally, the total penetrations to filter ratios increased with increasing particle size and for all particle sizes after pulling the head straps. In Group E, the total penetration to filter ratio had greatest increase for pulled staple condition and 1000 nm.

Leakage through the intact staple punctures was ~4 times greater for 200 and 500 nm particles, and ~9 times greater for 1000 nm particles, whereas leakage through the pulled staple punctures was ~5 times greater for 200 nm, ~6 times greater at 500 nm, and ~15 times greater for 1000 nm particles. Groups A and D had pulled and intact total penetration to leakage ratios near or below 2 for all conditions tested while Groups B and C had pulled and intact total penetration to filter ratios closer to 1.

At low flow, Group E had significantly greater pulled and intact total penetration to filter ratios at all particle sizes than all other respirator groups ($p<0.05$). While the staple punctures were intact Groups A and D had greater total penetration to filter ratios than Group C at 500 and 1000 nm particles sizes ($p<0.05$). Group D also had greater total penetration to filter ratios than Group B at 1000 nm particle size ($p<0.05$). When the staple punctures were pulled, Groups A and D had significantly greater total penetration to filter ratios than Groups B and C at all particle sizes ($p<0.05$).

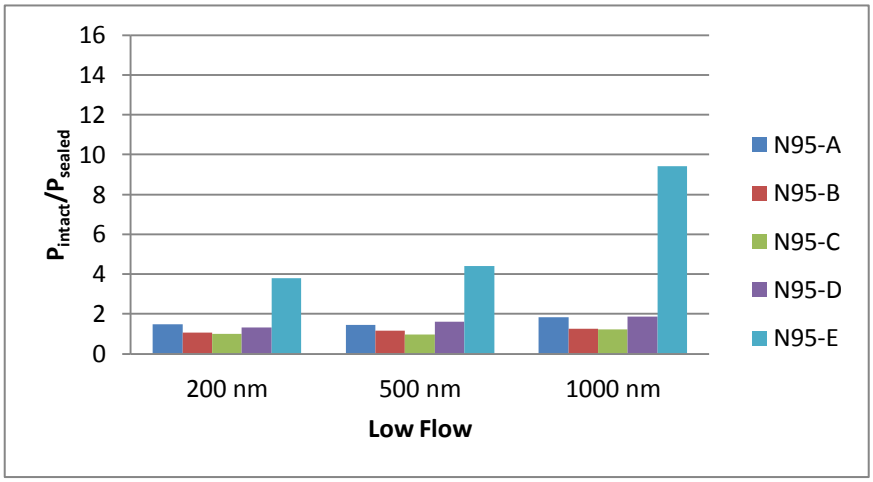

Figure 13. Total intact penetration to filter penetration ratios for the N95 FFR groups at 28 Liter/min constant flow rate.

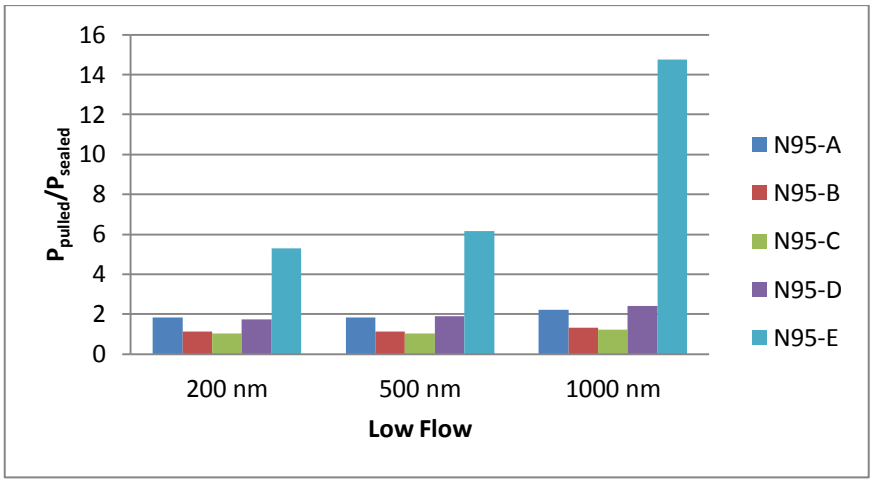

Figure 14. Total pulled penetration to filter penetration ratios for the N95 FFR groups at 28 Liter/min constant flow rate.

High Flow Total Penetration to Filter Ratios

Figures 15 and 16 show the mean P_{intact}/P_{sealed} and P_{pulled}/P_{sealed} ratios under high flow. The total penetrations to filter ratios decrease at the higher flow rate. Groups A, D, and E have a significant reduction of P_{pulled}/P_{sealed} ratio for 500 and 1000 nm particle sizes ($p<0.05$). In Groups D and E the difference is also significant for 200 nm ($p<0.05$). Similar to low flow, the total penetrations to filter ratios for high flow increased with increasing particle size and were greater when pulling the head straps. In Group E, the total penetration to filter ratio had the greatest increase for pulled staple condition at 1000 nm. Leakage through the intact staple punctures was ~3 times greater for 1000 nm particles, whereas leakage through the pulled staple punctures was ~5 times greater for 1000 nm particles. At high flow, all groups except for Group E had P_{pulled}/P_{sealed} ratios near 1 at all particle sizes. At high flow and pulled staple condition, Group E had significantly greater P_{pulled}/P_{sealed} and P_{intact}/P_{sealed} ratios than all other respirator groups at 500 and 1000 nm particle sizes ($p<0.05$).

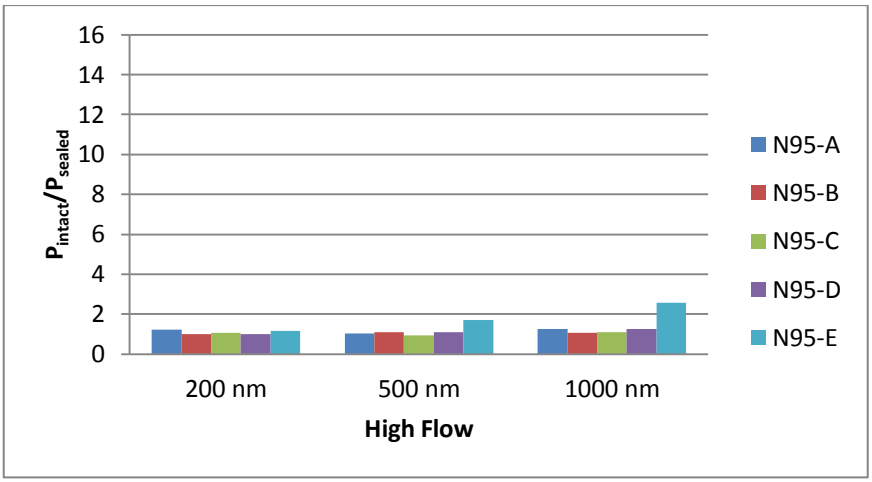

Figure 15. Total intact penetration to filter penetration ratios for the N95 FFR groups at 85 Liter/min constant flow rate.

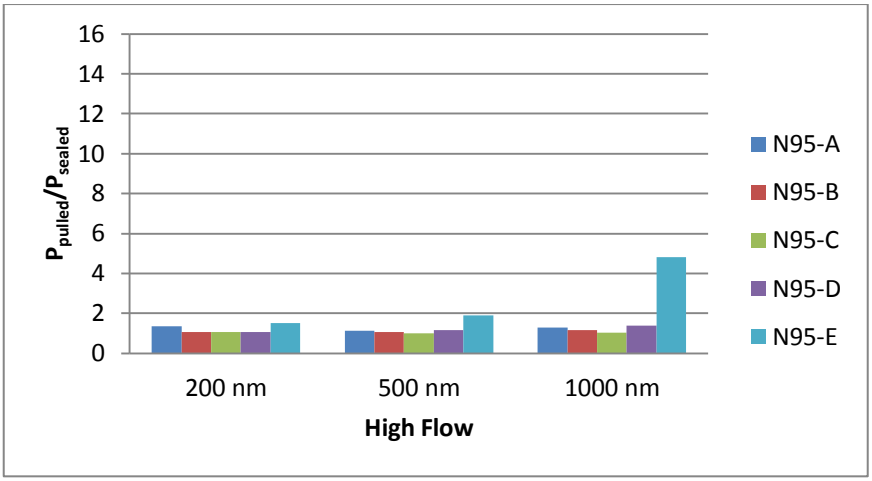

Figure 16. Total pulled penetration to filter penetration ratios for the N95 FFR groups at 85 Liter/min constant flow rate.

Protection Factors

The lowest PF (PF of 18) was in Group D for pulled staple condition, high flow and 200 nm (fig. 17). This was driven by poor filter efficiency. The greatest PF (PF of 934) was in Group E for sealed staple condition, low flow, and 1,000 nm. At low flow and 1000 nm, Group E had the greatest reduction of PF for pulled staple

punctures. Under these conditions, Group D offered a greater PF than Group E (PF of 94 to 61 respectively).

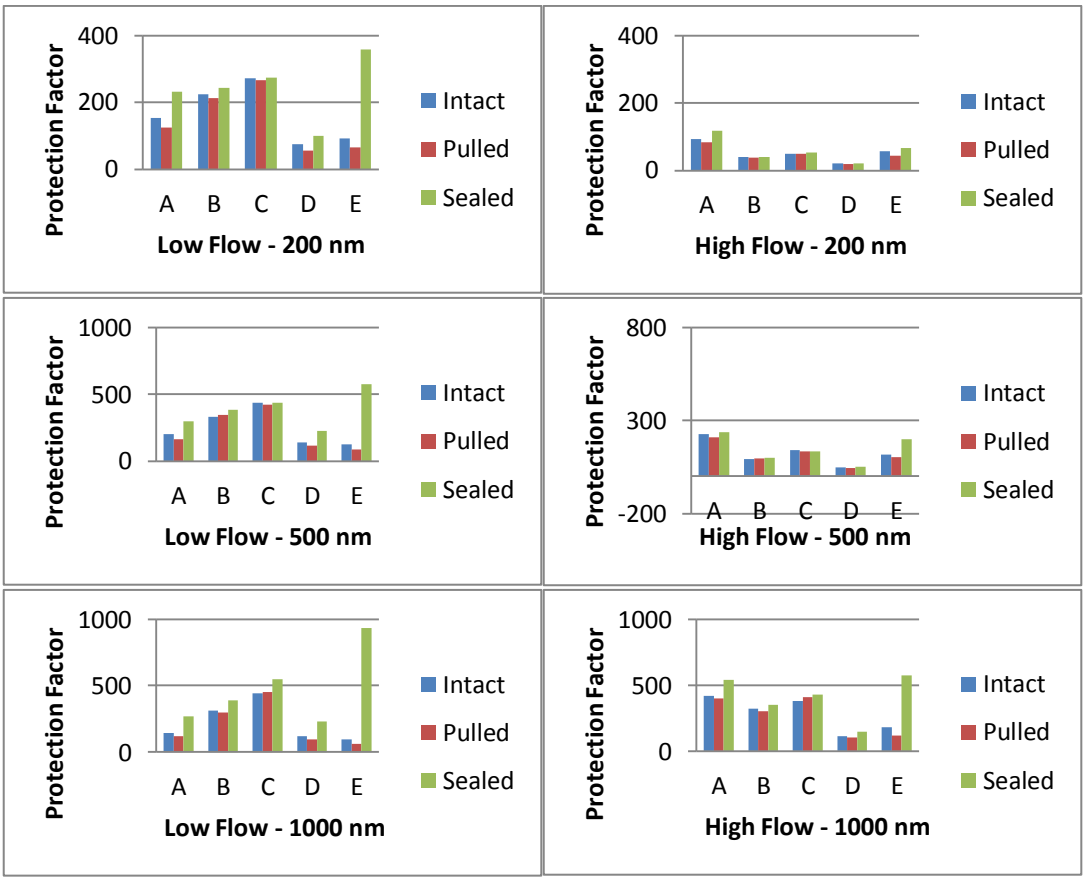

Figure 17. Protection Factors for the N95 FFR groups.

**Left column shows flow rate of 28 Liter/min and right column shows flow rate of 85 Liter/min. The top, middle, and bottom rows show the 200, 500, and 1,000 nm particle sizes.*

CHAPTER FIVE:

DISCUSSION

This chapter addresses the research objectives that were investigated in this study. All observations and determination of significance were made using 95% confidence intervals based on all the variables tested. The only marginal means considered were for the five subjects, representative of each respirator model.

Properties of a respirator, such as: manufacturer, filter thickness, packing density, fiber material, fiber size, and fiber charging methods may affect particle penetration through the filter of the respirator. Staple size and shape, staple attachment methods, staple puncture location, head strap position under staples, head strap length, head strap elasticity and head strap tension when pulled may affect leakage through the staple punctures. These factors were not considered in this study.

Main findings

All N95 respirator groups had the largest filter penetrations (P_{sealed}) at 200 nm particle size and high flow. Conversely, the largest mean leakages were observed at 1000 nm particle size and low flow. At low flow all P_{sealed} were under 1% and L_{pulled} were under 1.6%. At high flow, P_{sealed} were generally under 2.5% (except for Group D) and L_{pulled} were under 0.8%. The highest P_{pulled} values were generally below 3%.

Pulled Staple Punctures

The motion of pulling the head straps for respirator donning creates tension on the staple punctures which may further pull the fibers apart, enlarge a hole, or reduce the integrity of the fiber density in the immediate area. Generally speaking pulled leakages were greater than intact leakages. Intuitively, stretching the head straps would be expected to increase the leakage. However, the difference in leakage between intact and pulled staple conditions was not found to be significant under any of the conditions tested. Repetitive donning and doffing, pulling the staple puncture in different directions, continuous use over days or weeks, and stretching the head straps beyond what was evaluated in this study could increase L_{pulled} more than what was observed. That being said, the focus of the discussion will be on the leakages for pulled staple punctures.

P_{pulled} was greater than the P_{sealed} for two of the five N95 FFR models tested (Groups A and E) for all particle sizes at low flow ($p<0.05$). At high flow, this was only observed in Group E, for 1000 nm particle size ($p<0.05$). P_{pulled} in Group D were not significantly different than P_{sealed}. However, overall mean leakages in Group D were greater than those observed for Groups A, B and C. This suggests that two N95 respirator models (Groups A, and E) presented significant leakage with respect to their filter penetrations, and a third group (Group D) had greater mean leakages than the remaining Groups B and C ($p<0.05$) and marginally greater than leakage in Group A at all particle sizes and low flow. The effect of leakage on Groups A, D, and E was strongest at low flow and 1,000 nm particle size.

Poor filter efficiency in Group D may have contributed to the higher variability in total penetrations (intact and pulled) and filter penetrations (sealed) obtained. The

higher variability increases the range of the 95% CI which may explain why Group D does not have significantly lower penetration under sealed staple condition.

Staple Puncture Shape

Group E had the greatest observed leakage of all the respirator groups tested. The significant difference in leakage between Group E to Groups A and D are likely due, to differences among the staple punctures. When inspected with a light source behind the respirator, the areas adjacent to the staple punctures in Groups A and D were observed to have diminished fiber density, in comparison to other areas of the filter, as a result of pulling the head straps. The staple punctures in Group E tear a hole in the filter medium. Although this respirator had the greatest filter efficiency it had the greatest leakage through the staple punctures. Groups B and C did not have a visible difference in the fiber density near the staple punctures. Leakage is greater through circular holes than slit type holes because air flow resistance through slit type holes is greater (Brown, 1992). The FFR groups with staple punctures that reduce fiber density but do not create a hole are likely to share some resemblance to slit tip holes. Air flow is limited through the staple puncture leaks when a tear is not created in the filter medium, which suggests that leakage can be greatest on respirator models where the staple puncture creates a hole in the filter regardless of filter efficiency. The amount of leakage allowed into the breathing zone of the respirator can be expected to depend on the size of the tear created by the staple puncture.

Total Penetration to Filter Penetration Ratios

At low flow, the P_{pulled}/P_{sealed} ratios in Group E suggest that 1,000 nm particles were ~15 times more likely to leak than penetrate the filter, and 200 nm particles were ~5 times more likely to leak than penetrate the filter.

At high flow, the P_{pulled}/P_{sealed} ratios in Group E suggest ~5, 1000 nm particles leak for every particle that passes the filter and ~1.5, 200 nm particles leak for every particles that passes the filter. All other groups had total penetration to filter penetration ratios under ~2.5 for all conditions. This suggests that leakage through the staple punctures may increase up to 15 fold for large particles when the staple punctures tear a hole in the filter medium.

Protection Factors

All respirators in the study provided an PF greater than the OSHA APF of 10 for N95 disposable respirators. In Group E, a dramatic decrease in protection factor was observed when leakages through the staple punctures were significant. Group E had the greatest decrease in protection factor (from ~930 to ~60) followed by Group A (from ~270 to ~120) at 1000 nm and low flow rate. All other groups had a reduction in PF <135. With the head straps pulled, the PF of Group E was lower compared to Group D. This suggests that even a highly efficient N95 FFR with tears caused by staple punctures has the potential to offer less protection to the user than one that performs poorly when properly worn and fitted.

For pulled staple punctures and low flow, the PFs in Group E were less than 100 for all particles sizes. Lee, Grinshpun, and Reponen reported ~29% of tested N95 respirators (on human subjects) had PFs below 10 (2008). Furthermore, the remaining

~71% were below 50 (Reponen, Lee, Grinshpun, Johnson, and Mckay 2011). The reduction in PFs in Group E suggest that when, staple puncture create a hole in the filter medium, leakage through the staple punctures alone can reduce the PF close to values seen on human subjects.

N95 Certification

Group D had a P_{pulled} above the NIOSH requirement for N95 certification. This occurred at high flow and 200 nm (5.27%). Filtration efficiency of this model was poor (P_{sealed} of 4.93% at 200 nm) and was the driving mechanism for exceeding the 5% requirement by NIOSH for certification. Commercial sales of this FFR model were discontinued during the course of this study. At 85 LPM, the amount of leakage through the staples punctures on the five N95 FFR observed in this study would have minimal contribution in terms of failing N95 certification.

An Ideal Mass or Size for Particle Leakage

Mean leakage of 200 nm was generally greater than 1000 nm particles at high flow. However, the only significant leakage (Group E) relative to filter penetration at high flow was at 1000 nm. This could partially be attributed to the greater filter efficiency at the 1000 nm particle size (Rengasamy & Eimer 2011). Greater filter efficiency for larger particles reduces the variability of penetration and thus the range of the 95% CI yielding a significant difference for this particle size. This concept can be further explained with P_{pulled}/P_{sealed} ratio. As particle size increases, the denominator (filter penetration) becomes smaller due to enhanced filter efficiency for larger particle sizes. Although mean leakages for 1,000 nm were not significantly

greater than 200 nm at high flow, the total penetration to filter penetration ratios show that particle of 1,000 nm diameter had the greatest ability to leak relative to filter penetration when the staple punctures were pulled and created a hole in the filter.

The observed shift towards the smaller particle size at high flow can be attributed to a decrease in the effect of electrostatic attraction with increased flow rate through the filter (Chen et. al., 1990). Additionally, the higher particle size dependence of leakage towards smaller particles is due to the turbulence at the inlet of the leak and inside the leak itself (Chen & Willeke, 1992).

The streamlines inside leaks are suspected to continue inside of the breathing zone of the respirator (Myers, 1986), which suggests that the streamlines inside a leak flow predominantly in one direction. Hinds and Kraske report that flow through leaks increase as the size of the leak increases and as the total flow through the respirator decreases (1987). If the velocity of a particle inside a leak is increased in one direction, then the gained momentum of the particle may reduce the likelihood of its deviation from the leak streamline. This may be a possible explanation if the turbulence in the surrounding fibers of the leak is also reduced. At lower flow rates, particles of smaller size and mass are also more likely to be influenced by the electrostatic charges of nearby fibers, allowing only the larger particles through the leak.

Limitations

One of the serious limitations of this study is sample size. Due to the nature of the repeated measures design and the large quantity of variables and their respective sublevels, to obtain adequate power (80%) the sample size of each group would need

to be at least 30. A total of 125 additional respirators would have been required achieve adequate power. It is suspected that normality and homogeneity were not achieved with transformation of the data set due to the small sample size of this study. However, it was unfeasible to conduct testing on 130 subjects due to the extensive amount of labor required to test each subject.

Another limitation of this study was the range of the number of particle sizes used in the experiment which was dictated by the capacity of the particle counter used in this study. The particle sizes selected in this study covered the variations in the mechanisms of deposition that affect small and large particles. It is also expected that most exposures to particles, when not directly handling manufactured nanoparticles, are typically greater than 100 nm due to agglomeration or continuing condensation (Vincent & Clement, 2000).

Consistent Findings with the Available Literature

The leakage through the staple punctures of the N95 FFR groups that leaked have similar characteristics to that of FSL, especially when holes in the filter medium are created by the staple punctures. Leakage was observed to increase with increasing particle size and at lower flow rates as described by Cho et al. (2010). The findings of this study also agree that the fraction entering through the leak compared to the filter material increases with decreased flow rate (Chen et. al., 1990).

Total penetration to filter penetration ratios for the N95 FFR group with tears created by the staple punctures were in agreement with those reported by Grinshpun et. al. on human subjects (2009). Total penetration to filter penetrations on human subjects showed that 200 nm particles were ~10 times less likely to leak than 1,000 nm

particles (Grinshpun et. al., 2009). Similarly this study showed that 200nm particles were ~9.5 times less likely to leak than 1,000 nm. However, the leakage observed in Group E was approximately half of what reported for 1,000 nm particles by Grinshpun et. al. (2009).

The total penetrations to filter penetration ratios for all respirators under pulled staple conditions ranged from ~1 to ~14.8. Cho et. al., reported a similar range of 1.9 to 16.1 and suggested that FSL affects the level of protection more than filter penetration (2010). This is also in agreement with Coffey, Zhuang, Campbell, & Myers, who also found that FSL was a determining factor of total penetration for a respirator (1998). Coffey et. al. reported a FSL value of 2.4% (1998).

Chen and Willeke have commented on the shift on most leaking particles from larger particles at low flow to smaller particles at high flow, attributing it to higher turbulence at the inlet and inside the leak (1992). Chen et. al. suggests that the effect of electrostatic attraction is reduced as flow rate through the respirator increases (1990). The increase in leakage for 200 nm at high flow may be attributed to observation.

The findings of this study suggest that when staple punctures create a circular hole or tear in the filter medium, the behavior of the leaks through the staple punctures share similar characteristics of FSL, contribute significantly to amount of particles entering the breathing zone, and also alter the particle size distribution inside the respirator.

Contrary Findings with the Available Literature

In this study, the respirator group with the lowest filter penetration also had the greatest amount of leakage. This finding is contrary to what is reported by Rengasamy et. al., which suggests that filter penetrations indicate which respirator has the most potential to leak (2014). However, all leaks in his study were artificial and of a controlled size. The effect of staple puncture in this study is random and varied among the respirator models and, to a lesser extent, among the replicates.

Leakage reported by Grinshpun et. al., for 200nm was approximately 5% higher than the highest leakage observed in this study for the same particle size (2009). Leakage reported for the 1,000 nm particle size was approximately 1.5% higher. These leakages were from FSL on human subjects with a mean inhalation flow rate of 42 Liter/min (Grinshpun et. al., 2009).

Public Health Importance/Contributions

Identifying weaknesses in manufacturing methods and techniques for respiratory protective devices provides manufacturers with feedback on the limitations of their products and recommendations to improve the safety for consumers and users of these products.

In this study leakage through the staple punctures of N95 FFR were tested while the head straps were stretched, simulating a donned respirator. However, it is expected that leakage through the staple punctures in the field would increase due a greater stretching distance of the head straps to clear the users face and other personal protective equipment such as safety glasses which could likely place higher tension on the staple punctures than the methodology used in this study. Varying tensions in

different directions on the staple punctures have the potential to enlarge any tears or further reduce the density of the fibers in the immediate area.

This study suggests that cumulative leakage through staple punctures and face seal leaks have the potential to reduce the protection offered by the respirator. Under the conditions of this investigation it has been shown that leaks allow larger particles into the breathing zone. This is an important recognition because economical models of N95 FFR are more likely to have stapled head straps that puncture the filter. When purchasing N95 respirators for stock pile, it is likely that purchasers may select the least expensive option for compliance and purchase a model that likely punctures the filter material to anchor the head straps to the respirator.

Employers may also encourage the reuse of respirators in order to reduce costs. When respirators are used in a dusty environment, or for prolonged periods of time, they will begin to cake with dust. This will increase filtration efficiency, but if leaks are present, flow through these are expected to increase, allowing more particles to enter the breathing zone through of the respirator. Furthermore, the respirators that are reused for a long period of time expected to have greater cumulative tension placed on the staple punctures. In combination with a higher pressure drop it may allow more flow through the staple puncture leaks.

Future Research Directions

Filter penetrations for Groups A and E did not have a main effect for flow rate. It is likely that these groups had filter material with similar characteristics that allowed for better collection efficiency at high flow. It is possible that the pressure drop across

the filters of these respirator groups may be different than the remaining groups. This could increase the flow through the leaks. Further studies on staple puncture leakage should consider the effect of the pressure drop at across the respirator's filter.

The findings of this study suggest that leakage through staple punctures may occur at larger particle sizes. There is limited information on the effect of particle mass on leakage. Myers' findings suggest that as the size of the leak decreases, total leakage is reduced but the distribution of the aerosol shifts towards larger particle sizes (1986). The aerosols used in this study and most studies on filter penetration and leakage use a challenge aerosol of uniform density. Particles of larger mass may be less influenced by electrostatic attraction and are more likely to maintain their momentum when traveling through a streamline created by a leak. Investigating the effect of particle mass on leakage would be valuable since biological aerosols and aerosols encountered in industry may differ greatly in density. There is also a need to investigate particle size dependency of leakage on respirators that have their charge removed.

Conclusion

When staple punctures tear holes in the filter medium, the concentration of particles leaking through those openings is considerable and resembles face seal leakage. Flow rate and particle size have been found to influence leakage through the staple punctures. The greatest leakages occurred at 28 Liter/min and 1,000 nm. This suggests that a N95 with stapled head straps that tear or greatly reduce the density of the filter material are more prone to leaks when the work performed by the wearer

requires a low inhalation rate. The results of this study also suggest that when staple puncture leaks are present, the total penetration into the breathing zone is determined by the amount of particles entering through the leaks. Furthermore, because of the size dependency of the leaks at different flow rates, the particle size distribution inside the breathing zone of a respirator will vary according to the inhalation rate of the user. In the presence of a leak it would be expected that the particle size distribution inside the respirator would shift towards larger particle size. It is also likely for the staple puncture leaks to increase at lower flow rates. At higher inhalation rates at or above 85 Liter/min the amount of particles leaking through the staple punctures is reduced and the distribution is expected to shift towards the smaller particles, due to the increase in air turbulence in the leak and decreased collection efficiency of electrostatic attraction.

The tears and reduction in fiber density created by the pulled staple punctures were only visible when a bright light source was placed on the opposing side of the filter for inspection. Therefore it is recommended that a bright light source behind filter is used for inspection of tears and imperfections in the filter medium of a respirator.

The findings of this study suggest that stapling head straps directly onto the filtering material of a respirator has the potential to create leaks in amounts similar to that of face seal leaks. Consideration should be placed on whether respirators with stapled head straps that puncture the filter should be allowed on the market.

REFERENCES

Approval of Respiratory Protective Devices, 42 CFR § 84 (1995).

Balazy, A., Toivola, M., Reponen, T., Podgorski, A., Zimmer, A., Grinshpun, S.A. (2006). Manakin-based performance evaluation of N95 filtering-facepiece respirators challenged with nanoparticles. *Annals of Occupational Hygiene, 50*(3), 259–269. doi:10.1093/annhyg/mei058

Bergman, M.S., Viscusi, D.J., Zhaung, Z., Palmiero, A.J., Powell, J.B., Shaffer, R.E. (2012). Impact of multiple consecutive donning on filtering facepiece respirator fit. *American Journal of Infection Control, 40*(4), 375-380. doi:10.1016/j.ajic.2011.05.003

Brown, R.C. (1992). Review: Protection factors of respirators with special reference to dust respirators. *Journal of the International Society for Respiratory Protection,* 10, 5-33.

Brown, R.C. (1995). Protection against dust by respirators. *International Journal of occupational safety and ergonomics, 1*(1), 14-28.

Brosseau, L.M. (2010). Fit testing respirators for public health medical emergencies. *Journal of Occupational and Environmental Hygiene, 7*(11), 628-632. doi: 10.1080/15459624.2010.514782

Burgess G.L., Mashingaidze, M.T., (1999). Respirator leakage in the pharmaceutical industry of Northwest England. *Annals of Occupational Hygiene, 43*(8), 513-517.

CDC (2009, September 24). Interim recommendation for facemask and respirator use to reduce influenza A (H1N1) virus transmission. Retrieved from http://www.cdc.gov/h1n1flu/masks.htm

Chen, C.C., Ruuskanen, H., Pilacinski, W., Willeke, K. (1990). Filter and leak penetration characteristics of a dust and mist filtering facepiece. *American Industrial Hygiene Association Journal, 51*(12), 632-639.

Chen, C.C., Willeke, K. (1992). Characteristics of face seal leakage in filtering facepieces. *American Industrial Hygiene Associating, 53*(9), 533-539.

Cho, K.J., Reponen, T., Mckay, R., Shukla, R., Haruta, H., Sekar, P. (2010). Large particle penetration through N95 respirator filters and facepiece leaks with cyclic flow. *Annals of Occupational Hygiene, 54*(1), 68-77. doi:10.1093/annhyg/mep062

Coffey C.C., Zhuang Z., Campbell D.L., Myers, W.R. (1998). Quantitative fit testing of N95 respirators: Part II - Results, effect of filter penetration, fit test, and pass/fail criteria. *Journal of the International Society of Respiratory Protection, 16*, 25-36.

Coffey, C.C., Lawrence, R.B., Campbell, D.L., Zhuang, Z., Calvert, C.A., Jensen, P.A. (2004). Fitting characteristics of eighteen N95 filtering-facepiece respirators. *Journal of Occupational and Environmental Hygiene, (1*), 262-271. doi: 10.1080/15459620490433799

EPA (2011, September). Exposure Factors Handbook. Retrieved from http://www.epa.gov/ncea/efh/pdfs/efh-complete.pdf

Eshbaugh, J., Gardner, P., Richardson, A., & Hofacre, K., (2008). N95 and P100
respirator filter efficiency under high constant and cyclic flow. *Journal of Occupational and Environmental Hygiene, 6*(1), 52-61. doi:10.1080/15459620802558196

FDA (2010, June 22). Letter: Disposition of certain personal respiratory protection devices authorized for emergency use. Retrieved from http://www.fda.gov/MedicalDevices/Safety/EmergencySituations/ucm216890.htm

Grinshpun S.A., Haruta, H., Eninger, R.M., Reponen, T., McKay, R.T., Lee, S. (2009). Performance of an N95 filtering facepiece particulate respirator and a surgical mask during human breathing: Two pathways for particle penetration. *Journal of Occupational and Environmental Hygiene, 6*, 593-603. doi 10.1080/15459620903120086

Hinds, W.C., (1999). Aerosol technology: Properties, behavior, and measurement of airborne particles (2nd ed.). New York, NY: John Wiley & Sons, Inc.

Hinds, W.C., Kraske, G., (1987). Performance of dust respirator with facial seal leaks: I. Experimental. *American Industrial Hygiene Association*, *48*(10), 836-841.

Hogan, C.J., Kettleson, E.M., Lee, M.H., Ramaswami, B., Angenent, L.T., Biswas, P. (2005). Sampling methodologies and dosage assessment techniques for submicrometer and ultrafine virus aerosol particles. *Journal of Applied Microbiology, 99*(6), 1422-1434. doi:10.1111/j.1365-2672.2005.02720.x

Holton, P.M., Tackett, D.L., Willeke, K. (1987). Particle size dependent leakage and losses of aerosols in respirators. *American Industrial Hygiene Association Journal, 48*(10), 848-854.

Lee, S.A, Adhikari, A., Grinshpun, S.A., Mckay, R., Shukla, R., Zeigler, H.L., Reponen, T. (2005). Respiratory protection provided by N95 filtering facepiece respirators against airborne dust microorganisms in agricultural farms. *Journal of Occupational and Environmental Hygiene, 2*(11), 577-585. doi: 10.1080/15459620500330583

Lee, S., Grinshpun, S.A., Reponen, T. (2008). Respiratory performance offered by N95 respirators and surgical masks: human subject evaluation with NaCl aerosol representing bacterial and viral particle size range. *Annals of Occupational Hygiene, 52*(3), 177-185. doi: 10.1093/annhyg/men005

Lore, M.B., Sebastian, J.M., Brown, T.L., Viner, A.S., McCullough, N.V., Hinrichs, S.H. (2012). Performance of conventional and antimicrobial-treated filtering facepiece respirators challenged with biological aerosols. *Journal of Occupational and Environmental Hygiene, 9*(2), 69-80. doi: 10.1080/15459624.2011.640273

Lindsley, W.G., King, W.P., Thewlis, R.E., Reynolds, J.S., Panday, K., Cao, G., Szalajda, J.V. (2012a). Dispersion and exposure to a cough-generated aerosol in a simulated medical examination room. *Journal of Occupational and Environmental Hygiene, 9*(12), 681-690. doi:10.1080/15459624.2012.725986

Lindsley, W.G., Pearce, T.A., Hudnall, J.B., Davis, K.A., Davis, S.M., Fisher, M.A., Khakoo, R., Palmer, J.E., Clark, K.E., Celik, I., Coffey, C.C., Blachere, F.M., & Beezhold, D. H. (2012b). Quantity and size distribution of cough-generated aerosol particles produced by influenza patients during and after illness. *Journal of Occupational and Environmental Hygiene, 9*(7), 443-449. doi:10.1080/15459624.2012.684582

Martin, S.B., & Moyer, E.S. (2000). Electrostatic respirator filter media: filter efficiency and most penetrating particle size effects. *Applied Occupational and Environmental Hygiene, 15*(8), 609-617. doi:10.1080/10473220050075617

Mokler, B.V., White, R.K. (1983). Quantitative standard for exposure chamber integrity. *American Industrial Hygiene Association Journal, 44*, 292-295.

Mostofi, R., Noel, A., Haghighat, F., Bahloul, A., Lara, J., Cloutier, Y. (2012). Impact of two particle measurement techniques on the determination of N95 class respirator filtration performance against ultrafine particles. *Journal of Hazardous Materials, 217*(218), 51-57. doi:10.1016/j.jhazmat.2012.02.058

Myers, W.R., Allender, J., Plummer, R., Stobbe, T. (1986). Parameters that bias the measurement of airborne concentration within a respirator. *American Industrial Hygiene Association Journal*, 47(2), 106-114. doi: 10.1080/15298668691389423

NIOSH (2003, September). Respirator usage in private sector firms. Retrieved from http://www.cdc.gov/niosh/docs/respsurv/pdfs/respsurv2001.pdf

NIOSH (2009). Approaches to safe nanotechnology: Managing the health and safety concerns associated with engineered nanomaterials. Retrieved from http://www.cdc.gov/niosh/docs/2009-125/pdfs/2009-125.pdf

NIOSH (2014, March 13). Recommended guidance for extended use and limited reuse of N95 filtering facepiece respirators in healthcare settings. Retrieved from http://www.cdc.gov/niosh/topics/hcwcontrols/recommendedguidanceextuse.html

Noti, J.D., Lindsley, W.G., Blachere, F.M., Cao, G., Kashon, M.L., Thewlis, R.E., McMillen, C.M., King, W.P., Szalajda, J.V., & Beezhold, D.H. (2012). Detection of infectious influenza virus in cough aerosols generated in a simulated patient examination room. *Clinical Infectious Diseases, 54*(11),1569–1577. doi:10.1093/cid/cis237

Oberdorster, G., Oberdorster, E., Oberdorster, J. (2005). Nanotoxicology: An emerging discipline evolving from studies of ultrafine particles. *Environmental Health Perspectives, 113*(7), 823-839.

OSHA (2007). Pandemic influenza preparedness and response guidance for healthcare workers and healthcare employers. Retrieved from https://www.osha.gov/Publications/3328-05-2007-English.html

OSHA (2009). Assigned protection factors for the revised respiratory protection standard. Retrieved from https://www.osha.gov/Publications/3352-APF-respirators.pdf

Occupational Safety and Health Standards, 29 CFR § 1910.134 (2007).

Osborne, Jason (2002). Notes on the use of data transformations. *Practical Assessment, Research & Evaluation, 8*(6).

Plebani, C., Listrani, S., Tranfo, G., & Tombolini, F. (2012). Variation in penetration of submicrometric particles through electrostatic filtering facepieces during exposure to paraffin oil aerosol. *Journal of Occupational and Environmental Hygiene, 9*(9), 556-561. doi:10.1080/15459624.2012.709433

Raabe, O.G. (1968). The dilution of monodisperse suspensions for aerosolization. *American Industrial Hygiene Association, 29*, 439-443.

Rengasamy, S., King, W.P., Eimer, B.C., Shaffer, R.E. (2008). Filtration performance of NIOSH-approved N95 and P100 filtering facepiece respirators against 4 to *30 nanometer-size nanoparticles. Journal of Occupational and Environmental Hygiene, 5*(9), 556-564. doi: 10.1080/15459620802275387

Rengasamy, S., Eimer, B., & Shaffer, R. (2009). Comparison of nanoparticle filtration performance of NIOSH-approved and CE-marked particulate filtering facepiece respirators. *Annals of Occupational Hygiene, 53*(2), 117-128. doi:10.1093/annhyg/men086

Rengasamy, S., & Eimer, B. (2011). Total inward leakage of nanoparticles through filtering facepiece respirators. *Annals of Occupational Hygiene, 56*(5), 568-580. doi:10.1093/annhyg/meq096

Rengasamy, S., & Eimer, B. (2012). Nanoparticle penetration through filter media and leakage through face seal interface of N95 filtering facepiece respirators. *Annals of Occupational Hygiene, 56*(5), 568-580. doi:10.1093/annhyg/mer122

Reponen, T., Lee, S., Grinshpun, S.A., Johnson, E., McKay, R. (2011). Effect of fit testing on the protection offered by N95 filtering facepiece respirators against fine particles in a laboratory setting. *Annals of Occupational Hygiene, 55*(3), 264-271. doi:10.1093/annhyg/meq085

Schulte, P., Geraci, C., Zumwalde, R., Hoover, M., Castranova, V., Kuempel, E., Murashov, V., Vainio, H., Savolainen, K. (2008). Sharpening the focus on occupational safety and health in nanotechnology. *Scandinavian Journal of Work Environmental Health, 34*(6),471-478. doi:10.5271/sjweh.1292

Vincent, J.H., Clement, C.F., (2000). Ultrafine particles in workplace atmospheres. *Philosophical Transactions: Mathematical Physical and Engineering Sciences, 358*(1775), 2673-2682. doi: 10.1098/rsta.2000.0676

Viscusi, D.J., Bergman, M.S., Novak, D.A., Faulkner, K.A., Palmiero, A., Powell, J., Shaffer, R.E. (2011). Impact of three biological decontamination methods on filtering facepiece respirator fit, odor, comfort, and donning ease. *Journal of Occupational and Environmental Hygiene*, *8*(7), 426-436. doi: 10.1080/15459624.2011.585927

WHO (1999). Hazard prevention and control in the work environment: Airborne dust. doi: WHO/SDE/OEH/99.14

Zhuang, Z., Bradtmiller, B. (2005). Head-and-face anthropometric survey of U.S. respirator users. *Journal of Occupational and Environmental Hygiene, 2*(11), 567-576. doi:10.1080/15459620500324727

APPENDIX A:

STATISTICAL DIAGNOSIS

Table A1. Results for the Shapiro-Wilk Test of Normality.

Shapiro-Wilk Test of Normality

	Untransformed Data			Reciprocal Transformed Data		
	Statistic	df	Sig.	Statistic	df	Sig.
Group A	0.909	90	<0.001	0.976	90	0.101
Group B	0.726	90	<0.001	0.865	90	<0.001
Group C	0.711	90	<0.001	0.865	90	<0.001
Group D	0.776	90	<0.001	0.956	90	0.004
Group E	0.93	90	<0.001	0.924	90	<0.001
All Groups	0.731	450	<0.001	0.963	450	<0.001

Table A2. Results for the Levene Test of Homogeneity.

Test of Homogeneity of Variance

	Untransformed Data				**Reciprocal Transformed Data**			
	Levene Statistic	df1	df2	Sig.	Levene Statistic	df1	df2	Sig.
Group A	1.961	4	85	0.108	0.544	4	85	0.704
Group B	0.43	4	85	0.787	0.996	4	85	0.414
Group C	1.934	4	85	0.112	1.159	4	85	0.335
Group D	0.169	4	85	0.954	1.378	4	85	0.248
Group E	1.214	4	85	0.311	0.316	4	85	0.867
All Groups	5.581	24	425	<0.001	1.958	24	425	0.005
	2.366*	24*	425*	<.0001*	0.702*	24*	425*	0.851*

*values based on median

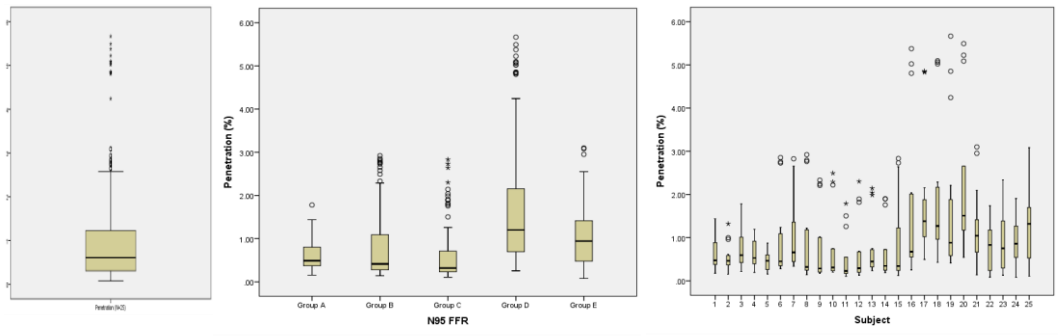

Figure A1. Untransformed penetration values (n=450).

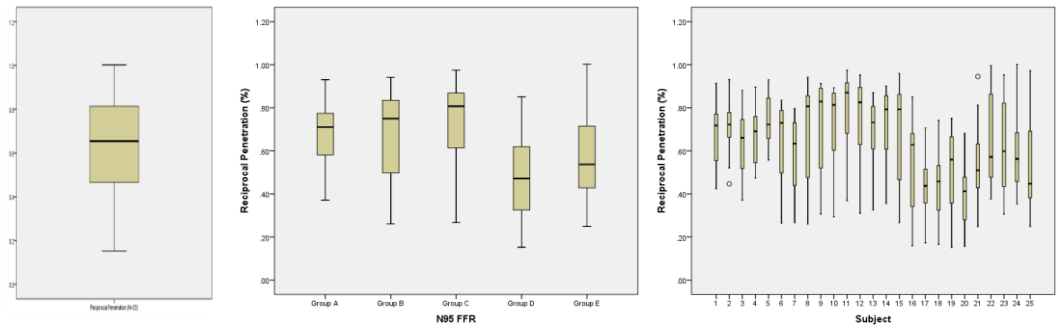

Figure A2. Reciprocal transformed penetration values (n=450).

APPENDIX B:

RESULTS

Table B1. Mean penetration, standard error, and 95% CI intervals for each N95 group and marginal means of all groups.

Respirator Group	Staple Condition	Particle Size	Flow Rate	Penetration (%)	Std. Error	95% Confidence Interval	
						Lower Bound	Upper Bound
A	Intact	200 nm	Low	0.65	0.02	0.48	0.87
			High	1.07	0.02	0.86	1.32
		500 nm	Low	0.49	0.01	0.43	0.56
			High	0.44	0.00	0.44	0.45
		1,000 nm	Low	0.69	0.02	0.53	0.89
			High	0.24	0.01	0.20	0.28
	Pulled	200 nm	Low	0.80	0.03	0.56	1.15
			High	1.20	0.04	0.81	1.82
		500 nm	Low	0.61	0.03	0.44	0.83
			High	0.48	0.02	0.39	0.59
		1,000 nm	Low	0.84	0.03	0.60	1.16
			High	0.25	0.02	0.17	0.35
	Sealed	200 nm	Low	0.43	0.03	0.29	0.60
			High	0.84	0.04	0.53	1.32
		500 nm	Low	0.33	0.02	0.26	0.42
			High	0.42	0.02	0.33	0.53
		1,000 nm	Low	0.37	0.02	0.27	0.49
			High	0.19	0.01	0.15	0.23

Table B1 (Continued). Mean penetration, standard error, and 95% CI intervals for each N95 group and marginal means of all groups.

Respirator Group	Staple Condition	Particle Size	Flow Rate	Penetration (%)	Std. Error	95% Confidence Interval	
						Lower Bound	Upper Bound
B	Intact	200 nm	Low	0.44	0.04	0.25	0.72
			High	2.53	0.01	2.20	2.94
		500 nm	Low	0.30	0.04	0.15	0.51
			High	1.09	0.03	0.78	1.53
		1,000 nm	Low	0.32	0.04	0.17	0.52
			High	0.31	0.02	0.23	0.40
	Pulled	200 nm	Low	0.47	0.04	0.29	0.71
			High	2.65	0.01	2.36	2.99
		500 nm	Low	0.29	0.03	0.18	0.42
			High	1.05	0.03	0.80	1.40
		1,000 nm	Low	0.34	0.04	0.17	0.57
			High	0.33	0.02	0.23	0.45
	Sealed	200 nm	Low	0.41	0.03	0.25	0.62
			High	2.50	0.01	2.19	2.87
		500 nm	Low	0.26	0.03	0.16	0.38
			High	0.99	0.02	0.79	1.24
		1,000 nm	Low	0.26	0.03	0.13	0.42
			High	0.29	0.01	0.23	0.35
C	Intact	200 nm	Low	0.37	0.02	0.28	0.47
			High	2.02	0.02	1.52	2.78
		500 nm	Low	0.23	0.03	0.13	0.35
			High	0.71	0.02	0.55	0.90
		1,000 nm	Low	0.23	0.03	0.10	0.39
			High	0.26	0.02	0.20	0.34
	Pulled	200 nm	Low	0.37	0.02	0.27	0.49
			High	2.03	0.02	1.68	2.48
		500 nm	Low	0.24	0.02	0.17	0.31
			High	0.74	0.04	0.49	1.11
		1,000 nm	Low	0.22	0.03	0.10	0.38
			High	0.24	0.02	0.18	0.32
	Sealed	200 nm	Low	0.36	0.03	0.24	0.52
			High	1.88	0.03	1.35	2.71
		500 nm	Low	0.23	0.02	0.17	0.30
			High	0.75	0.03	0.50	1.09
		1,000 nm	Low	0.18	0.03	0.07	0.32
			High	0.23	0.01	0.18	0.30

Table B1 (Continued). Mean penetration, standard error, and 95% CI intervals for each N95 group and marginal means of all groups.

Respirator Group	Staple Condition	Particle Size	Flow Rate	Penetration (%)	Std. Error	95% Confidence Interval	
						Lower Bound	Upper Bound
D	Intact	200 nm	Low	1.33	0.02	1.01	1.78
			High	4.85	0.01	4.39	5.41
		500 nm	Low	0.72	0.04	0.44	1.15
			High	2.07	0.01	1.75	2.48
		1,000 nm	Low	0.83	0.06	0.43	1.56
			High	0.87	0.03	0.59	1.27
	Pulled	200 nm	Low	1.75	0.03	1.23	2.61
			High	5.27	0.00	4.87	5.72
		500 nm	Low	0.85	0.04	0.53	1.37
			High	2.18	0.01	1.87	2.59
		1,000 nm	Low	1.06	0.06	0.56	2.05
			High	0.96	0.04	0.61	1.53
	Sealed	200 nm	Low	1.00	0.02	0.77	1.31
			High	4.93	0.00	4.76	5.12
		500 nm	Low	0.44	0.02	0.35	0.55
			High	1.89	0.01	1.63	2.21
		1,000 nm	Low	0.43	0.03	0.29	0.61
			High	0.69	0.01	0.62	0.76
E	Intact	200 nm	Low	1.08	0.02	0.90	1.31
			High	1.74	0.03	1.26	2.51
		500 nm	Low	0.81	0.02	0.63	1.04
			High	0.85	0.04	0.56	1.30
		1,000 nm	Low	1.08	0.03	0.76	1.53
			High	0.56	0.06	0.25	1.09
	Pulled	200 nm	Low	1.53	0.03	1.15	2.08
			High	2.28	0.03	1.62	3.39
		500 nm	Low	1.11	0.02	0.87	1.42
			High	0.97	0.05	0.58	1.63
		1,000 nm	Low	1.64	0.03	1.16	2.41
			High	0.85	0.04	0.53	1.37
	Sealed	200 nm	Low	0.28	0.03	0.16	0.43
			High	1.50	0.02	1.13	2.03
		500 nm	Low	0.17	0.02	0.09	0.27
			High	0.50	0.06	0.20	1.04
		1,000 nm	Low	0.11	0.01	0.07	0.14
			High	0.17	0.03	0.08	0.28

Table B1 (Continued). Mean penetration, standard error, and 95% CI intervals for each N95 group and marginal means of all groups.

Respirator Group	Staple Condition	Particle Size	Flow Rate	Penetration (%)	Std. Error	95% Confidence Interval	
						Lower Bound	Upper Bound
Mean	Intact	200 nm	Low	0.70	0.01	0.63	0.77
			High	2.05	0.01	1.89	2.23
		500 nm	Low	0.47	0.01	0.42	0.54
			High	0.90	0.01	0.82	0.99
		1,000 nm	Low	0.56	0.02	0.48	0.65
			High	0.41	0.02	0.35	0.47
	Pulled	200 nm	Low	0.83	0.01	0.74	0.93
			High	2.27	0.01	2.07	2.51
		500 nm	Low	0.55	0.01	0.49	0.61
			High	0.95	0.01	0.85	1.06
		1,000 nm	Low	0.67	0.02	0.58	0.78
			High	0.47	0.01	0.41	0.53
	Sealed	200 nm	Low	0.46	0.01	0.40	0.52
			High	1.86	0.01	1.68	2.06
		500 nm	Low	0.28	0.01	0.25	0.31
			High	0.79	0.02	0.69	0.90
		1,000 nm	Low	0.26	0.01	0.22	0.30
			High	0.29	0.01	0.26	0.31

Table B2. Mean leakage, standard error, and 95% CI intervals for each N95 group and marginal means of all groups.

Respirator Group	Staple Condition	Particle Size	Flow Rate	Leakage (%)	Std. Error	95% Confidence Interval	
						Lower Bound	Upper Bound
A	Intact	200 nm	Low	0.23	0.04	0.12	0.36
			High	0.17	0.06	0.03	0.36
		500 nm	Low	0.15	0.04	0.06	0.26
			High	0.04	0.03	-0.03	0.12
		1,000 nm	Low	0.31	0.04	0.18	0.47
			High	0.06	0.05	-0.04	0.17
	Pulled	200 nm	Low	0.36	0.04	0.21	0.55
			High	0.30	0.07	0.09	0.62
		500 nm	Low	0.28	0.03	0.18	0.40
			High	0.06	0.04	-0.03	0.15
		1,000 nm	Low	0.46	0.04	0.30	0.67
			High	0.07	0.04	-0.03	0.19
B	Intact	200 nm	Low	0.05	0.04	-0.03	0.14
			High	0.05	0.06	-0.06	0.20
		500 nm	Low	0.05	0.04	-0.03	0.14
			High	0.12	0.03	0.04	0.21
		1,000 nm	Low	0.07	0.04	-0.02	0.17
			High	0.02	0.05	-0.07	0.13
	Pulled	200 nm	Low	0.07	0.04	-0.03	0.18
			High	0.15	0.07	-0.02	0.38
		500 nm	Low	0.03	0.03	-0.04	0.11
			High	0.07	0.04	-0.02	0.17
		1,000 nm	Low	0.09	0.04	-0.01	0.20
			High	0.05	0.04	-0.04	0.17
C	Intact	200 nm	Low	0.02	0.04	-0.06	0.11
			High	0.14	0.06	0.01	0.32
		500 nm	Low	0.02	0.04	-0.05	0.11
			High	0.01	0.03	-0.06	0.08
		1,000 nm	Low	0.05	0.04	-0.04	0.15
			High	0.04	0.05	-0.05	0.15
	Pulled	200 nm	Low	0.02	0.04	-0.07	0.12
			High	0.11	0.07	-0.05	0.33
		500 nm	Low	0.02	0.03	-0.05	0.09
			High	0.01	0.04	-0.06	0.11
		1,000 nm	Low	0.04	0.04	-0.04	0.14
			High	0.02	0.04	-0.07	0.13

Table B2 (Continued). Mean leakage, standard error, and 95% CI intervals for each N95 group and marginal means of all groups.

Respirator Group	Staple Condition	Particle Size	Flow Rate	Leakage (%)	Std. Error	95% Confidence Interval	
						Lower Bound	Upper Bound
D	Intact	200 nm	Low	0.31	0.04	0.19	0.46
			High	0.06	0.06	-0.05	0.21
		500 nm	Low	0.28	0.04	0.17	0.42
			High	0.18	0.03	0.09	0.28
		1,000 nm	Low	0.40	0.04	0.26	0.59
			High	0.19	0.05	0.07	0.34
	Pulled	200 nm	Low	0.74	0.04	0.51	1.06
			High	0.29	0.07	0.08	0.59
		500 nm	Low	0.42	0.03	0.30	0.57
			High	0.28	0.04	0.16	0.43
		1,000 nm	Low	0.64	0.04	0.44	0.91
			High	0.27	0.04	0.14	0.45
E	Intact	200 nm	Low	0.79	0.04	0.57	1.09
			High	0.25	0.06	0.09	0.45
		500 nm	Low	0.62	0.04	0.44	0.85
			High	0.30	0.03	0.20	0.43
		1,000 nm	Low	0.96	0.04	0.69	1.35
			High	0.37	0.05	0.21	0.58
	Pulled	200 nm	Low	1.23	0.04	0.86	1.78
			High	0.79	0.07	0.41	1.45
		500 nm	Low	0.93	0.03	0.71	1.21
			High	0.44	0.04	0.29	0.63
		1,000 nm	Low	1.53	0.04	1.08	2.24
			High	0.68	0.04	0.45	0.99
Mean	Intact	200 nm	Low	0.23	0.03	0.13	0.35
			High	0.13	0.03	0.07	0.20
		500 nm	Low	0.19	0.03	0.11	0.29
			High	0.12	0.02	0.07	0.18
		1,000 nm	Low	0.29	0.04	0.17	0.43
			High	0.12	0.03	0.06	0.20
	Pulled	200 nm	Low	0.36	0.05	0.21	0.56
			High	0.29	0.04	0.17	0.43
		500 nm	Low	0.26	0.04	0.15	0.40
			High	0.15	0.03	0.08	0.23
		1,000 nm	Low	0.40	0.05	0.24	0.61
			High	0.18	0.03	0.09	0.29

Table B3. Mean total penetration to filter penetration ratios for each N95 group and the marginal means of all groups.

Respirator Group	Staple Condition	Particle Size	Flow Rate	Total Penetration to Filter Penetration Ratio	Std. Error	95% Confidence Interval	
						Lower Bound	Upper Bound
A	Intact	200 nm	Low	1.47	0.06	1.19	1.90
			High	1.24	0.04	1.07	1.45
		500 nm	Low	1.47	0.05	1.20	1.86
			High	1.03	0.05	0.89	1.22
		1,000 nm	Low	1.83	0.05	1.49	2.34
			High	1.27	0.07	0.99	1.72
	Pulled	200 nm	Low	1.83	0.05	1.49	2.36
			High	1.35	0.05	1.12	1.67
		500 nm	Low	1.82	0.03	1.56	2.17
			High	1.13	0.04	0.99	1.31
		1,000 nm	Low	2.22	0.04	1.82	2.82
			High	1.29	0.06	1.05	1.64
B	Intact	200 nm	Low	1.07	0.06	0.90	1.30
			High	1.02	0.04	0.89	1.17
		500 nm	Low	1.15	0.05	0.97	1.40
			High	1.10	0.05	0.94	1.31
		1,000 nm	Low	1.26	0.05	1.08	1.51
			High	1.08	0.07	0.86	1.41
	Pulled	200 nm	Low	1.14	0.05	0.98	1.35
			High	1.06	0.05	0.91	1.27
		500 nm	Low	1.12	0.03	1.01	1.27
			High	1.07	0.04	0.93	1.23
		1,000 nm	Low	1.32	0.04	1.15	1.54
			High	1.15	0.06	0.95	1.44
C	Intact	200 nm	Low	1.01	0.06	0.85	1.22
			High	1.07	0.04	0.94	1.24
		500 nm	Low	0.97	0.05	0.83	1.15
			High	0.94	0.05	0.82	1.10
		1,000 nm	Low	1.24	0.05	1.06	1.48
			High	1.11	0.07	0.88	1.45
	Pulled	200 nm	Low	1.03	0.05	0.89	1.21
			High	1.07	0.05	0.91	1.27
		500 nm	Low	1.03	0.03	0.93	1.15
			High	1.00	0.04	0.88	1.14
		1,000 nm	Low	1.22	0.04	1.07	1.41
			High	1.03	0.06	0.86	1.26

Table B3 (Continued). Mean total penetration to filter penetration ratios for each N95 group and the marginal means of all groups.

Respirator Group	Staple Condition	Particle Size	Flow Rate	Total Penetration to Filter Penetration Ratio	Std. Error	95% Confidence Interval	
						Lower Bound	Upper Bound
D	Intact	200 nm	Low	1.32	0.06	1.08	1.66
			High	0.98	0.04	0.87	1.13
		500 nm	Low	1.60	0.05	1.29	2.05
			High	1.10	0.05	0.94	1.30
		1,000 nm	Low	1.86	0.05	1.52	2.39
			High	1.24	0.07	0.97	1.68
	Pulled	200 nm	Low	1.75	0.05	1.43	2.23
			High	1.07	0.05	0.91	1.28
		500 nm	Low	1.91	0.03	1.63	2.29
			High	1.15	0.04	1.01	1.34
		1,000 nm	Low	2.42	0.04	1.96	3.14
			High	1.37	0.06	1.11	1.77
E	Intact	200 nm	Low	3.80	0.06	2.51	7.40
			High	1.16	0.04	1.01	1.36
		500 nm	Low	4.42	0.05	2.85	9.26
			High	1.69	0.05	1.38	2.15
		1,000 nm	Low	9.43	0.05	4.80	121.40
			High	2.58	0.07	1.73	4.73
	Pulled	200 nm	Low	5.29	0.05	3.35	11.87
			High	1.53	0.05	1.25	1.93
		500 nm	Low	6.17	0.03	4.18	11.41
			High	1.91	0.04	1.57	2.39
		1,000 nm	Low	14.76	0.04	6.61	999.77
			High	4.83	0.06	2.88	13.38
Mean	Intact	200 nm	Low	1.41	0.05	1.18	1.71
			High	1.09	0.02	1.02	1.17
		500 nm	Low	1.49	0.05	1.24	1.84
			High	1.13	0.03	1.03	1.26
		1,000 nm	Low	1.84	0.05	1.50	2.35
			High	1.33	0.04	1.14	1.57
	Pulled	200 nm	Low	1.62	0.05	1.34	2.04
			High	1.19	0.03	1.09	1.31
		500 nm	Low	1.66	0.05	1.36	2.10
			High	1.19	0.03	1.08	1.33
		1,000 nm	Low	2.06	0.05	1.63	2.73
			High	1.44	0.05	1.20	1.77

Table B4. Mean protection factors for each N95 group and the marginal means of all groups.

Respirator Group	Staple Condition	Particle Size	Flow Rate	Protection Factor	Std. Error	95% Confidence Interval	
						Lower Bound	Upper Bound
A	Intact	200 nm	Low	153.09	0.02	115.25	206.30
			High	93.61	0.02	75.51	115.66
		500 nm	Low	202.39	0.01	178.31	230.87
			High	226.87	0.00	223.95	229.84
		1,000 nm	Low	144.99	0.02	112.03	189.54
			High	418.36	0.01	362.75	488.84
	Pulled	200 nm	Low	124.32	0.03	87.29	178.61
			High	83.25	0.04	55.10	123.10
		500 nm	Low	163.94	0.03	120.63	227.41
			High	208.11	0.02	169.78	258.69
		1,000 nm	Low	119.65	0.03	86.13	167.10
			High	399.67	0.02	289.06	595.50
	Sealed	200 nm	Low	233.12	0.03	166.24	343.02
			High	118.43	0.04	75.66	187.04
		500 nm	Low	300.32	0.02	239.44	387.01
			High	235.41	0.02	188.13	300.59
		1,000 nm	Low	268.42	0.02	202.22	370.43
			High	538.48	0.01	444.35	671.21
B	Intact	200 nm	Low	225.05	0.04	138.96	402.91
			High	39.46	0.01	34.00	45.36
		500 nm	Low	330.32	0.04	197.74	665.07
			High	91.85	0.03	65.32	127.94
		1,000 nm	Low	312.11	0.04	190.91	597.99
			High	323.45	0.02	251.45	431.43
	Pulled	200 nm	Low	213.92	0.04	140.41	348.97
			High	37.72	0.01	33.41	42.29
		500 nm	Low	345.53	0.03	238.50	547.95
			High	95.02	0.03	71.42	125.72
		1,000 nm	Low	296.85	0.04	175.75	597.55
			High	300.61	0.02	220.55	432.13
	Sealed	200 nm	Low	243.85	0.03	161.83	397.23
			High	40.08	0.01	34.87	45.68
		500 nm	Low	386.60	0.03	262.19	636.59
			High	101.30	0.02	80.68	126.97
		1,000 nm	Low	391.04	0.03	237.37	790.18
			High	350.40	0.01	289.28	433.70

Table B4 (Continued). Mean protection factors for each N95 group and the marginal means of all groups.

Respirator Group	Staple Condition	Particle Size	Flow Rate	Protection Factor	Std. Error	95% Confidence Interval	
						Lower Bound	Upper Bound
C	Intact	200 nm	Low	272.72	0.02	212.66	360.37
			High	49.51	0.02	35.99	65.83
		500 nm	Low	438.82	0.03	287.73	776.00
			High	141.75	0.02	110.64	183.14
		1,000 nm	Low	441.30	0.03	259.37	978.80
			High	380.26	0.02	294.61	512.11
	Pulled	200 nm	Low	267.41	0.02	202.12	367.43
			High	49.33	0.02	40.28	59.54
		500 nm	Low	424.45	0.02	327.13	577.74
			High	134.38	0.04	90.28	203.59
		1,000 nm	Low	451.17	0.03	261.98	1034.76
			High	410.71	0.02	315.49	561.06
	Sealed	200 nm	Low	274.23	0.03	190.63	422.61
			High	53.28	0.03	36.89	73.83
		500 nm	Low	437.62	0.02	336.13	599.12
			High	134.09	0.03	91.58	199.52
		1,000 nm	Low	548.11	0.03	315.95	1340.27
			High	426.47	0.01	338.28	558.02
D	Intact	200 nm	Low	75.39	0.02	56.33	99.43
			High	20.60	0.01	18.50	22.77
		500 nm	Low	139.09	0.04	86.76	229.66
			High	48.31	0.01	40.28	57.24
		1,000 nm	Low	121.10	0.06	64.30	233.44
			High	115.21	0.03	78.96	168.83
	Pulled	200 nm	Low	57.04	0.03	38.36	81.16
			High	18.99	0.00	17.49	20.52
		500 nm	Low	117.07	0.04	73.21	188.80
			High	45.77	0.01	38.65	53.61
		1,000 nm	Low	94.40	0.06	48.77	177.26
			High	103.70	0.04	65.26	163.95
	Sealed	200 nm	Low	100.10	0.02	76.50	130.59
			High	20.27	0.00	19.55	20.99
		500 nm	Low	226.85	0.02	181.19	289.56
			High	52.86	0.01	45.33	61.17
		1,000 nm	Low	230.46	0.03	163.58	340.90
			High	145.45	0.01	131.35	161.29

Table B4 (Continued). Mean protection factors for each N95 group and the marginal means of all groups.

Respirator Group	Staple Condition	Particle Size	Flow Rate	Protection Factor	Std. Error	95% Confidence Interval	
						Lower Bound	Upper Bound
E	Intact	200 nm	Low	92.18	0.02	76.47	110.80
			High	57.34	0.03	39.87	79.48
		500 nm	Low	123.92	0.02	96.52	159.77
			High	117.15	0.04	77.06	179.28
		1,000 nm	Low	93.01	0.03	65.23	131.36
			High	179.62	0.06	91.43	406.76
	Pulled	200 nm	Low	65.42	0.03	48.09	87.05
			High	43.92	0.03	29.50	61.71
		500 nm	Low	90.08	0.02	70.35	114.69
			High	103.17	0.05	61.50	171.86
		1,000 nm	Low	61.03	0.03	41.45	86.50
			High	117.44	0.04	73.25	189.97
	Sealed	200 nm	Low	358.07	0.03	230.32	640.36
			High	66.63	0.02	49.38	88.11
		500 nm	Low	576.79	0.02	366.77	1119.14
			High	199.23	0.06	96.12	511.44
		1,000 nm	Low	934.20	0.01	707.53	1335.16
			High	574.67	0.03	351.08	1221.58
Mean	Intact	200 nm	Low	143.21	0.01	129.50	158.60
			High	48.68	0.01	44.76	52.82
		500 nm	Low	210.72	0.01	186.11	239.81
			High	111.02	0.01	101.39	121.58
		1,000 nm	Low	177.91	0.02	153.32	207.58
			High	243.64	0.02	211.75	282.58
	Pulled	200 nm	Low	120.38	0.01	107.91	134.37
			High	43.96	0.01	39.84	48.33
		500 nm	Low	181.91	0.01	162.92	203.76
			High	105.22	0.01	94.18	117.54
		1,000 nm	Low	148.42	0.02	127.73	173.06
			High	214.60	0.01	189.22	244.70
	Sealed	200 nm	Low	217.99	0.01	193.18	247.24
			High	53.87	0.01	48.48	59.65
		500 nm	Low	357.14	0.01	320.91	400.04
			High	126.89	0.02	111.29	144.87
		1,000 nm	Low	387.21	0.01	335.92	451.87
			High	346.26	0.01	318.89	377.37

APPENDIX C:

MAIN EFFECT AND INTERACTIONS INCLUDING STAPLE

ANOVA Results by Group N=5

Three of the five groups had a main effect for staple (Group A (p=.038), Group D (p=.014) & Group E (p=.004). Three way interaction between staple×size×flow was only significant in Group A (p=.040). Two way interaction between staple×flow were observed in Group D (p=.024) & group E (p=.001). Two way interaction between staple×size was only observed in group C (p=.039). However, Group C did not have a main effect for staple. Group B did not have a main effect for staple or any interaction terms including staple.

3 Way Interactions

Group A: Staple×Size×Flow

At low flow, sealed penetration was significantly lower than pulled and intact penetrations for 500 and 1000 nm particles. At high flow penetration for 1000 nm particles were significantly different for all staple conditions.

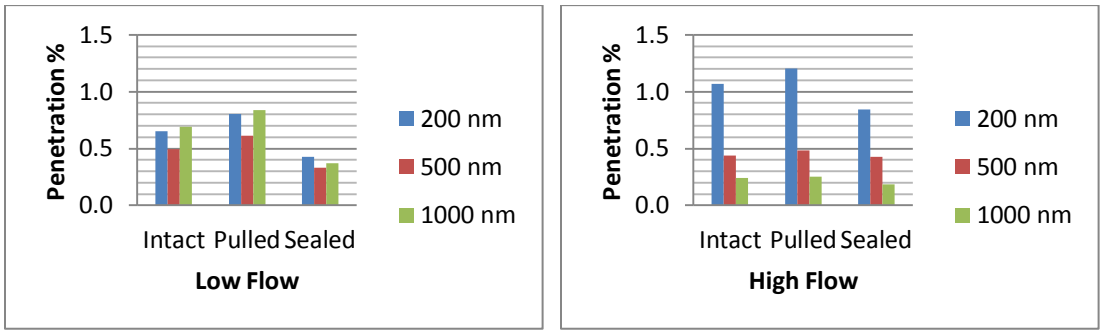

Figure C1. Mean penetrations for N95 Group A interaction (staple×size×flow).

Table C1. Mean penetration, standard error, and 95% CI intervals for N95 Group A interaction (staple×size×flow).

Respirator Group	Staple Condition	Particle Size	Flow Rate	Penetration (%)	Std. Error	95% Confidence Interval	
						Lower Bound	Upper Bound
A	Intact	200 nm	Low	0.653	0.025	0.485	0.868
			High	1.068	0.019	0.865	1.324
		500 nm	Low	0.494	0.01	0.433	0.561
			High	0.441	0.001	0.435	0.447
		1,000 nm	Low	0.69	0.023	0.528	0.893
			High	0.239	0.008	0.205	0.276
	Pulled	200 nm	Low	0.804	0.031	0.56	1.146
			High	1.201	0.035	0.812	1.815
		500 nm	Low	0.61	0.027	0.44	0.829
			High	0.481	0.017	0.387	0.589
		1,000 nm	Low	0.836	0.029	0.598	1.161
			High	0.25	0.02	0.168	0.346
	Sealed	200 nm	Low	0.429	0.027	0.292	0.602
			High	0.844	0.04	0.535	1.322
		500 nm	Low	0.333	0.016	0.258	0.418
			High	0.425	0.018	0.333	0.532
		1,000 nm	Low	0.373	0.021	0.27	0.495
			High	0.186	0.01	0.149	0.225

2 Way Interactions

Group C: Staple×Size

Penetrations generally increase with decrease in particle size at all staple conditions. For all staple conditions, penetrations for 200 nm are than penetrations for 500 and 1,000 nm. Penetrations for 500 nm were only significantly different than 1,000 nm for sealed staple condition.

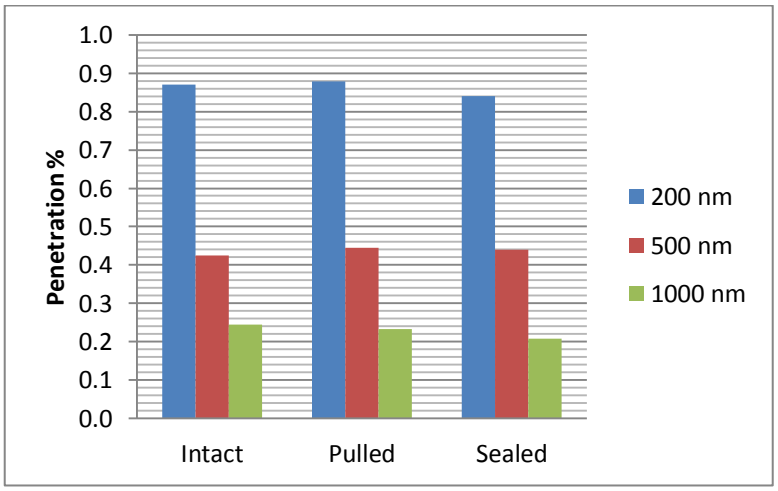

Figure C2. Mean penetrations for N95 Group C interaction (staple×size).

Table C2. Mean penetration, standard error, and 95% CI intervals for N95 Group C interaction (staple×size).

Respirator Group	Staple Condition	Particle Size	Penetration (%)	Std. Error	95% Confidence Interval	
					Lower Bound	Upper Bound
C	Intact	200 nm	0.87	0.02	0.73	1.04
		500 nm	0.43	0.02	0.33	0.54
		1000 nm	0.25	0.02	0.17	0.33
	Pulled	200 nm	0.88	0.02	0.74	1.05
		500 nm	0.44	0.03	0.33	0.58
		1000 nm	0.23	0.02	0.15	0.33
	Sealed	200 nm	0.84	0.03	0.63	1.12
		500 nm	0.44	0.02	0.33	0.58
		1000 nm	0.21	0.02	0.14	0.28

Group D and E: Staple×Flow

In both groups D and E, penetration at high flow was greater than low flow when staple condition was intact and sealed. When the staples were pulled, penetrations under low and high flow were not significantly different. In group D, there were no significant changes in penetration among staple conditions under a single flow rate. In Group E, penetrations at low flow for intact and pulled staple conditions were greater than sealed penetrations.

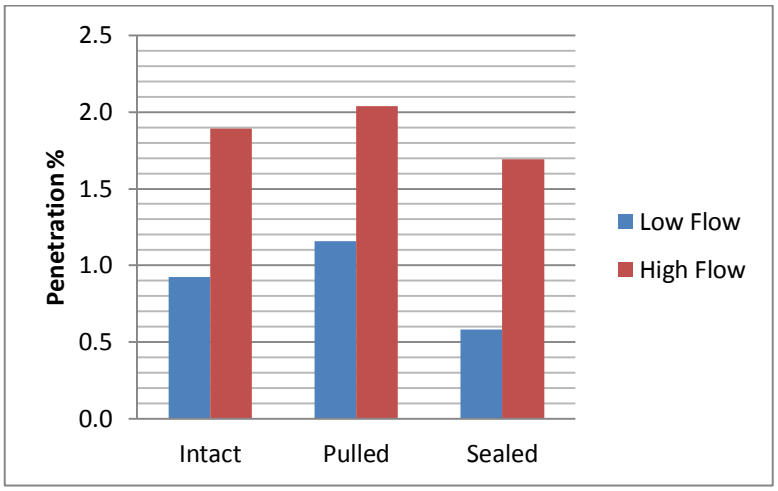

Figure C3. Mean penetrations for N95 Group D interaction (staple×flow).

Table C3. Mean penetration, standard error, and 95% CI intervals for N95 Group D interaction (staple×flow).

Respirator Group	Staple Condition	Flow Rate	Penetration (%)	Std. Error	95% Confidence Interval	
					Lower Bound	Upper Bound
D	Intact	Low	0.92	0.04	0.59	1.45
		High	1.89	0.02	1.56	2.33
	Pulled	Low	1.16	0.05	0.72	1.91
		High	2.04	0.02	1.66	2.54
	Sealed	Low	0.58	0.03	0.44	0.76
		High	1.69	0.01	1.55	1.85

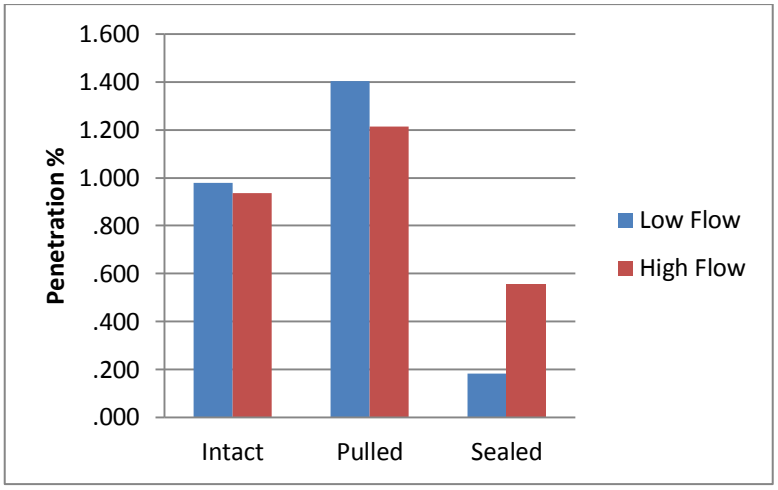

Figure C4. Mean penetrations for N95 Group E interaction (staple×flow).

Table C4. Mean penetration, standard error, and 95% CI intervals for N95 Group E interaction (staple×flow).

Respirator Group	Staple Condition	Flow Rate	Penetration (%)	Std. Error	95% Confidence Interval	
					Lower Bound	Upper Bound
E	Intact	Low	0.98	0.04	0.77	1.24
		High	0.94	0.02	0.62	1.42
	Pulled	Low	1.40	0.05	1.05	1.90
		High	1.21	0.02	0.81	1.85
	Sealed	Low	0.18	0.03	0.11	0.27
		High	0.56	0.01	0.35	0.85

Comparison of Respirators

Using the Bonferonni method to evaluate difference among groups, significantly different levels of penetration were observed among the different N95 FFR models. Group D had the poorest filter performance of all groups tested ($p<.001$) and ($p=.004$) when compared with group E. Group E performed significantly different than Groups A, C and D ($p=.041$), ($p=.004$) and ($p=.004$). The marginal mean penetration for Groups A, B and C did not differ significantly.

Main effect for staple

Staple condition had a significant main effect on 4 of the 5 respirator groups tested. Greatest mean penetrations where observed for all respirators during pulled staple condition. In groups A and D and E, pulled penetration were greater than sealed penetration ($p=.015$) and ($p=.009$) and ($p=.001$), respectively. In Groups D and E, intact penetrations were also significantly greater than sealed penetrations ($p=.038$) and ($p=.005$), respectively. Group E had the largest decrease in penetration after sealing the staple punctures.

Group D had the greatest mean penetration for all staple conditions and had a larger sealed penetration value than the rest of the groups. This suggests Group D had the worst performing N95 FFR model. Group E had the second highest mean penetrations for intact and pulled staple conditions. However, for sealed staple conditions Group E had the lowest penetration. This suggests that Group E had the best performing N95 FFR model.

Interaction Terms for All Groups

Staple × Flow

Filter penetrations were generally greater during high flow. Although group E had an overall penetration greater than group A and C, at low flow, group E had the lowest penetration of all respirators for sealed staple condition. Significant differences in penetration between the staple conditions were observed in groups A, D, and E.